Rare Earth Element-bearing Fluorite Deposits of Turkey: an overview

Hüseyin Öztürk[1]*, Sinan Altuncu[2], Nurullah Hanilçi[1], Cem Kasapçi[1], Kathryn M. Goodenough[3]

[1]Istanbul University-Cerrahpaşa, Department of Geological Engineering, Avcılar Campus, 34320 Avcılar, Istanbul, Turkey

[2]Ömer Halisdemir University, Department of Geological Engineering, 51100 Niğde, Turkey

[3]British Geological Survey, Lyell Centre, Research Avenue South, Edinburgh EH14 4AP, UK

*e-mail: ozturkh@istanbul.edu.tr

Abstract

Rare Earth Element (REE)-bearing fluorite deposits in Turkey occur in association with Cenozoic post-collisional alkaline-carbonatite systems and can be divided into three groups: (1) carbonatite-associated; (2) those associated with subalkaline to alkaline magmatic rocks of Cretaceous to Cenozoic age; and (3) those in sedimentary successions, typically in areas dominated by limestone. Some of these deposits show significant enrichment in the REE, especially the Kızılcaören deposit which has average REE grades of almost 30,000 ppm; others have very low REE contents but have potential fluorite resources.

The homogenization temperature and salinity values of fluid inclusions in these deposits vary between 600°C to 150 °C, and 10-65 wt.% NaCl eq., respectively. The carbonatite-associated deposits have the highest bulk REE contents and are LREE-enriched. As a general feature, the REE contents of the fluorite deposits decrease with decreasing homogenization temperatures and salinity of the fluorite fluid inclusions. Fluorite ore chemistry indicates that a plot of Nb+Ta versus total REE differentiates the carbonatite- hosted from the alkali intrusive- hosted and carbonate- hosted deposits. Beyond the cooling and/or dilution of the fluids, REE and fluorite deposition was driven by changes in pH, instead of change in Eh, according to our geostatistical treatment. The chondrite-normalized rare earth element patterns of each group of deposits show some similar features, indicating that the REE in the fluorite are independent of their host

lithology, but reflect the magmatic systems from which they were derived. Overall, the F-REE deposits of the Anatolides-Taurides in Turkey are considered to be largely related to the post-collisional magmatic systems, but with variable contributions of fluids from other sources.

Key words: Fluorite, REE, Geochemistry, fluid inclusion, Turkey

1. Introduction

The rare earth elements (REE) and fluorspar (fluorite) have been identified as critical materials by the European Commission (EC, 2014). Deposits of the REE are found in a range of geological settings, including carbonatites; alkaline to peralkaline igneous rocks; hydrothermal deposits; heavy mineral placers and weathered ion adsorption clay deposits (Dill, 2010; Chakhmouradian and Wall, 2012; Weng et al., 2015; Goodenough et al., 2016; Verplanck and Hitzman, 2016). In many of these settings, the REE may be associated with fluorite.

Economic fluorite deposits are most commonly formed through hydrothermal processes, occurring in a range of different associations. These associations include: (1) REE-bearing carbonatite (e.g. Kızılcaören, Turkey, Özgenç, 1993a, Nikiforov et al., 2014; Bayan Obo, China, Yang et al., 2009., Xu et al., 2012, Smith et al., 2015; Maoniuping, China, Liu at al., 2018; Verplanck, et al., 2014; Dalucao, Lizhuang and Muluozhai, China, Liu and Hou, 2017; Okorusu, Namibia, Bühn et al., 2002; (2) alkaline to peralkaline granitoids (e.g. Gallinas Mountains, Williams-Jones et al., 2000, St Lawrence granite, Strong et al., 1984); (3) Highly differentiated S - type granites (e.g. Voznesenka deposit, Russia, Sato et al., 2003), (4) sedimentary sequences, particularly passive margin carbonates (e.g. Southern Alpine, Italy, Hein et al., 1990; Encantada- Buenavista, Mexico, Gonzalez-Partida et al., 2003; Komshecheh, Iran, Rajabzadeh, 2007., Asturias, Spain, Sanchez et al., 2009) and, (5) active continental margin settings (Dill et al., 2016). REE deposits can be magmatic, hydrothermal and even supergene in origin. In contrast, fluorite deposits may form in a range of host lithologies, but they are generally formed from hydrothermal fluids (Dill, 2010), which may come from igneous or sedimentary sources (Richardson and Holland 1979). Fluorine-rich alkaline melts derived from the mantle can rise to shallow levels in the continental crust without solidification, because their high volatile contents decrease the melt viscosity (Edgar and Arima, 1985; Dingwell et al., 1985; Lange, 1994; Dingwell and Hess, 1998; Giordano et al., 2008). Chloride and sulphate complexes are important for transport of the REE, whereas fluoride ions tend to promote REE mineral deposition (Migdisov and Williams-Jones, 2014); hence carbonatite or alkaline rock-hosted fluorite deposits may also include economic grades of REE (Hess et al., 1995; Smith and Henderson 2000; Williams-Jones et al., 2000; Gammons et al., 2002). Fluorite deposits may also form in or around large S -type granites, and may be sourced by partial melting of F-rich aluminosilicates in metasedimentary rocks, including mica and amphibole (Goldschmidt, 1954). Fluorides also make stable complexes with Sn (Bensurov and Kurril'chrkove, 1966; Thomas et al., 2005) and U (Kimberly, 1979) during the late magmatic hydrothermal phase, and thus a F+U+Sn ore association is also recognised. The origin of fluorine for replacement and vein- type fluorite deposits in sedimentary hosts is more variable. Fluorine and associated elements may have been derived directly from the sedimentary rocks, from deeper crustal rocks by metamorphic fluids circulating at depth, or from magmatic sources (Hein et al., 1990; Levresse et al., 2003; Sanchez et al., 2009).

The Anatolides of Turkey lie within the Alpine orogenic belt and include a range of different types of fluorite and fluorite –bearing REE deposits, including carbonatite-hosted (Hatzl, 1992; Nikiforov et al., 2014; Berg, 2018), pegmatitic (Dill, 2015), alkaline magmatic-hosted and limestone-hosted types (Şaşmaz and Yavuz 2007; Altuncu, 2009). Although some individual studies have been carried out on these deposits (Kaplan, 1977a; Yaman, 1985; MTA, 1989, Özgenç, 1993a; Özgenç, 1993b; Uçurum et al., 1997; Uras et al., 2004; Şaşmaz et al., 2005a; Şaşmaz et al., 2005b; Genç, 2006; Şaşmaz and Yavuz, 2007), there has thus far been no comparative investigation of Turkey's REE - bearing fluorite deposits. This paper reviews these REE - bearing fluorite deposits, and aims to understand whether there are common controls on their history, on the basis of their geological setting, geochemistry, host lithologies and fluid inclusion characteristics. A second objective is the comparison of Turkish REE- bearing fluorite deposits with other well-known deposits of the Alpine – Himalayan orogenic belt, as well as other world class deposits in different tectonic settings.

2. Regional geological setting of the REE-bearing fluorite deposits

The geological framework of Turkey consists of three main tectonic units (Fig. 1): from north to south these are the Pontides (Eurasian Plate), Anatolides-Taurides (Anatolian Microplate) and Arabian Plate (Şengör and Yılmaz 1981; Moix et al., 2008). The Anatolian microplate and Arabian plate together represent part of the northern margin of Gondwana (Gürsu et al., 2015). These three tectonic units were amalgamated during the Mesozoic and Cenozoic, along east- west trending ophiolitic suture belts. The North Anatolian Suture Zone (NASZ), also known as the İzmir-Ankara-Erzincan suture, is of Upper Cretaceous- Eocene age and occurs between the Pontides and Anatolides-Taurides

(Şengör and Yılmaz 1981). The South Anatolian Suture zone (SASZ), of Eocene age, occurs between the Anatolides-Taurides and the Arabian Plate (Fig. 1).

The geology of the eastern Pontides consists of Palaeozoic aged epi-metamorphic rocks of the Kargı and Tokat massifs which are intruded by Permian granitoids including the Gümüşhane granite (Yılmaz et al., 1997). The western Pontides has a Pan- African basement of Proterozoic age (Okay, 2008). Thick volcano-sedimentary successions of Mesozoic age, formed in active arcs, occur in the eastern Black Sea region, and post-collisional Eocene volcanics occur along the eastern Black Sea coast. Fluorite- REE deposits are not known from the volcano-sedimentary rock units of the Pontides.

The Anatolian Microplate (Anatolides-Taurides) was assembled during the closure of the Palaeo Tethys and collided with the Pontides in the Late Cretaceous to Eocene (Moix et al., 2008). The Anatolides-Taurides consist of high-grade metamorphic massifs, the Menderes, Kırşehir, and Bitlis massifs (Fig. 1), which are overlain by thick carbonates of Palaeozoic and Mesozoic age in the Taurus Mountains. The metamorphic massifs and carbonates are cut by post-collisional alkaline intrusives of Cenozoic age (the central Anatolian granitoids; Boztuğ, 1998a; Boztuğ 1998b; Boztuğ et al., 2007; Kuşcu et al., 2013) and associated hydrothermal activity has formed fluorite veins. Oligo-Miocene aged post-collisional molasse and evaporites, which include hydrothermally formed celestine deposits (Tekin et al., 2002) in gypsum series evaporite deposits, are widespread within an east-west- trending belt in central Anatolia. Miocene aged horst–graben structures and associated calc-alkaline and alkaline magmatism occur especially in Western Anatolia (Altunkaynak et al., 2012a; Altunkaynak et al., 2012b, Okay and Satır, 2006). REE-bearing fluorite deposits in this area are associated with Paleocene to Miocene carbonatite to alkaline magmatism, related to retreat and roll-back of the Hellenic arc (Aysal, 2015).

South of the SASZ, the Arabian Plate comprises a thick sequence of Palaeozoic and Mesozoic age passive margin sedimentary rocks and Cenozoic foreland basin sediments (Fig 1).

3. Methods

The mineralogical composition of the fluorite ores was investigated by petrographic examination of thin sections and by XRD (X-Ray Diffraction). The XRD studies were performed in Istanbul University-Cerrahpaşa, Department of Geology, with a Rigaku D/Max-2200 model instrument using a Cu Kα tube with settings of 40 kV, 20 mA and 2 theta. The minerals were identified using the database from the Jade 6.5 software. 123 samples of fluorite were then selected, using a binocular microscope, for geochemical analysis, which was performed at ACME Laboratories (Vancouver, Canada). Samples were ground finer than 700 mesh for the chemical analyses. The major oxides (SiO_2, TiO_2, Al_2O_3, MnO, MgO, CaO, K_2O, Na_2O, P_2O_5) and LOI of the samples were analysed by inductively coupled plasma-atomic emission spectrometry (ICP-AES) after $LiBO_2$ fusion. The trace elements were analysed by inductively coupled plasma-mass spectrometry (ICP–MS), with rare earth and incompatible elements determined from $LiBO_2$ fusion, and precious and base metals determined from an aqua-regia digestion. Fluorine was analysed in fusion, analysis by specific ion electrode method.

The loss on ignition was measured by weighing the samples before and after ignition at 1000 °C. The total iron concentration is determined as Fe_2O_3. All of the samples were analysed together with STD-SO-18, an international standard. For F, samples were analysed together with STD-C3 standard. The Boynton, (1984) chondrite values have been used for normalization.

Fluid inclusion studies were carried out on doubly polished thin sections of the fluorite minerals. The measurements were made with a Linkham THMG600 (at Istanbul University, Department of Geology, Turkey) heating–freezing stage mounted on an Olympus optical microscope fitted with video camera and monitor. Heating and freezing measurements were undertaken using standard techniques as described by Roedder (1984) and Shepherd et al., (1985). Accuracy was ±0.5°C for the heating stage and ±0.2°C for the freezing stage according to synthetic fluid inclusion standards obtained from Fluid Inclusion Laboratory Leoben.

Microthermometric measurements of fluid inclusions were carried out on 80–120 µm thick, doubly polished fluorite wafers using standard techniques (Roedder, E., 1984; Shepherd et al., 1985) at the fluid inclusion laboratory in Istanbul University, using a Linkam THMSG-600 heating–freezing stage. The stage was calibrated using pure H_2O, CO_2 and H_2O-NaCl standards and potassium dichromate. According to replicate measurements, the accuracy is estimated to be in the order of ±5° for heating and ±0.4° for freezing measurements. During the measurements, the values of homogenisation temperature (T_h), eutectic temperature (T_e), last-ice melting temperature ($T_{m\text{-}ice}$), and melting temperature of salts ($T_{m\text{-}NaCl}$, $T_{m\text{-}KCl}$) were measured. Liquid nitrogen was used for freezing.

4. REE-bearing fluorite deposits

The REE-bearing fluorite deposits of Turkey have been divided into three major types on the basis of the host rocks (Altuncu, 2009). These are: (i) carbonatite-associated deposits (ii) alkaline-intrusive-hosted deposits, and (iii) sedimentary carbonate-hosted deposits. This classification is followed in the present study.

Fieldwork was carried out at 3 actively mined fluorite deposits and 10 mineralization locations where small-scale mining activity has stopped. Host rocks, ore geometry, and alteration features of the deposits are described below. During the field study more than 500 samples were collected from these deposits.

4.1. Carbonatite-associated REE - fluorite deposits

Kızılcaören (KO): The Kızılcaören deposit is enriched in F, Ba, REE and Th. It is located in western Turkey, approximately 40 km from Eskişehir city (Fig.1). The exploration and exploitation licence for the deposit currently belongs to a government company, Etimaden. Investigation of the deposit has focused on Th and REE; estimated resources are 0.38 Mt of ThO_2 ore with an average grade of 0.212 wt.% and 4.67 Mt of REE (Ce+ La+ Nd+Y) ores with an average grade of 2.78 wt.% (Kaplan 1977a). Although some estimates have suggested a few tens of millions tons of barite and fluorite with a total grade of 40 % (Kaplan, 1977b) there is no formal fluorite and barite resource calculation.

The geology of the Kızılcaören region comprises an accretionary complex melange, separated by a major fault zone from serpentinised ultramafic rocks that include podiform chromite beds and are cut by young subvolcanic necks. The melange series comprises weakly metamorphosed sandstone, breccia, schist, limestone and volcanic blocks of Triassic-Jurassic age. The fault zone between the melange series and serpentinite provided a pathway for phonolite and carbonatitic melts with emplacement of associated F- Ba-REE-Th veins in the Oligocene (25-24 Ma), (Nikiforov et al., 2014).

The ore deposit comprises Th- bearing bastnäsite-barite-fluorite veins and lenses, occurring within the metasedimentary rocks of the melange (Fig. 2a; Table 1). Stocks of phonolite, and dykes of carbonatite, occur close to the zone of mineralization and all formed at c.24- 25 Ma (Nikiforov et al., 2014). Evidence of alkaline metasomatism ('fenitisation'; Elliott et al., 2018) occurs in the host rocks to the carbonatite.

The ore zone consists of tabular to lensoid layered ore bodies and, more rarely, vertical to sub-vertical veins. The banded tabular ore is characterised by interbanding of purple fluorite, barite, and bastnäsite, with some cross-cutting barite veins (Fig. 3a). Manganese and iron oxides are abundant within the upper part of the deposit, which has been substantially affected by weathering and oxidation.

The tabular ore lenses are up to a few tens of metres in thickness and a few tens to hundreds of metres in length and have gentle to moderate dips (5 - 20 degrees). Contacts with the wall-rocks are generally sharp, and in some areas the wall-rocks show evidence of intense silicification and brittle fracturing prior to ore lens formation. The rare near-vertical ore veins, which are typically finer-grained, can be considered as the feeder system of the banded ore lenses. Many independent ore lenses have been defined in boreholes down to 600 meters depth (Eti Maden Operations General Directorate, pers comm).

Within the ore lenses, fluorite occurs as large crystals up to a few cm in size, most commonly dark purple and less frequently white, greenish or purple blue. The ore mineralogy and paragenesis has been previously described by Stumpfl and Kırıkoğlu, 1985; Gultekin et al., 2003; and Nikiforov et al., 2014). An earlier stage comprises coarse-grained fluorite, barite, phlogopite and pyrite, with a second phase richer in barite, calcite and bastnäsite. Other minerals recognised in the ore lenses include K-feldspar, monazite, pyrochlore, Nb- rutile, and (in surface outcrops) the oxidation products florencite, hematite and limonite (Table 1). Nikiforov et al., (2014) suggest that the primary Mn carbonate, Fe carbonate and Ca carbonate minerals in the ore have been dissolved and oxidised during supergene alteration, with the ore becoming porous and banded (Fig. 3b).

Kuluncak (KUL): The Kuluncak F-REE-Th deposit, also known as Sofular, is located 4 km south of Başören village (Kuluncak-Malatya) in central-eastern Turkey (Fig. 1). The geology of the area is dominated by a Cretaceous to Cenozoic volcano-sedimentary succession, including some thick limestones (Leo et al., 1978). The fluorite deposit occurs as veins, veinlets and replacement lenses in the limestone adjacent to an intrusive stock of nepheline syenite that contains carbonatite veins (Özgenç and Kibici, 1994) (Fig. 2b). Cretaceous to Cenozoic sedimentary units are overlain by Miocene aged basaltic lava and cut by trachytic domes. The ore includes blue, light and dark purple fluorite (Fig.3c and 3d), bastnäsite, apatite, siderite, calcite, britholite and quartz (Table 1). The britholite contains 57% REE and 2.68 % ThO_2 (Özgenç and Kibici, 1994). The region was investigated for Th deposits by the MTA in the 1960s and further exploration drilling is currently being undertaken by MTA.

4.2. Alkaline intrusive-hosted REE- bearing fluorite deposits

Bayındır (BY)

This deposit is located between Yozgat and Kırşehir in central Anatolia (Fig. 1). In this region, the large Cenozoic Bayındır syenite-diorite pluton (part of the Central Anatolian granitoid suite) cuts pre-Mesozoic basement and the overlying Mesozoic to Cenozoic sedimentary units (Koç et al., 2003). The fluorite veins occur as stockworks and fracture filling veins, 30 to 80 cm thick, within the syenitic rocks. The ore consists of coarse-grained purple, green and yellowish fluorites (Fig. 4a, b). Well-developed argillic alteration around the fluorite veins is characterized by quartz, clay and minor calcite. The measured and indicated resources were defined as 0.125 Mt of fluorite by MTA (1979) and the deposit is currently mined underground. Yaman (1984) and Koç et al. (2003) found low homogenization temperatures for fluid inclusions in fluorite (65-120 °C) and relatively low total REE contents in fluorite, up to 250 ppm.

İsahocalı (IH): The deposit is located 20 km northeast of Kaman, also within the Bayındır pluton. The fluorite mineralization zone comprises individual veins 30 to 80 cm in thickness and between 15 m and 50 m in length, and the ore zone extends for approximately 200 m, within the altered alkali syenite (Fig. 2c). The ore comprises banded veins filled by green and purple fluorite, and quartz (Fig. 4c). Resources were estimated as 0.01 Mt of ore with 67 wt.% fluorite (MTA, 1979). Koç et al., (2003) measured total REE in fluorites as 60-270 ppm and observed a flat REE pattern with negative Ce and positive Eu anomalies. They found homogenization temperatures of fluid inclusions in fluorite varying from 180 to 290 °C.

Cangıllı (CA): The Cangıllı (CA) fluorite deposit is located north of Cangıllı village (Yerköy-Yozgat). The fluorite occurs as a NE-trending vein within an alkali syenite intrusion, part of the Bayındır syenite pluton (Fig. 2c). The ore vein is approximately 150 m long and 10 to 25 cm thick, and consists of green and purple coarse-grained fluorite with calcite (Fig. 4d). Resource estimates are 0.05 Mt at 69 wt.% fluorite as measured, and 0.2 Mt as indicated resource (MTA, 1979). The deposit was mined sporadically in the 1960s.

Akçakent (AKC): The Akçakent (AKC) fluorite deposit in central Anatolia forms veins within the Cenozoic Yılanlı syenites (Koç and Reçher, 2001). The zone of veining extends for approximately 450 m within the altered syenite (Fig. 2c) and at the tectonic contact between the syenite and associated gabbro (Table 1). The ore veins are typically 70-80 cm thick and oriented N-NW. Fluorites occur as vein fill, and as breccia cement in fractured syenites. Quartz and rare barite accompany green and purple fluorite in the ore paragenesis (Fig. 4 e, f).

Divriği (DIV): The Divriği fluorite deposit in eastern-central Turkey (Fig. 1) is approximately 10 km NE of the important iron ore deposits of Divriği (Öztürk et al., 2016). In this area, ophiolitic rocks are cut by A-type granitoids that were intruded during the late Cretaceous (Boztuğ et al., 2007). The fluorite deposit comprises a complex ore zone that is enriched in F+U+Cu (Table 1). The ore zone was investigated by MTA in 1958 with three boreholes and trenches for uranium. A gallery 50 m in length and two shafts were opened in the ore body. Coarse-grained, green fluorites occur as vein fillings within alkali granite, with argillic alteration around the ore vein (Fig. 4g, h). The ore zone includes discrete veins and stockwork veins trending ENE (Table 1; Fig. 2 d), extends approximately 300 m along strike, and is 0.6 to 1 m in total thickness. The estimated fluorite resource is 0.036 Mt on the basis of the limited studies conducted by MTA. The ore includes fluorite, chalcopyrite, pyrite, galena, arsenopyrite, bismuthinite, dolomite and quartz (Table 1).

4.3. Carbonate-hosted REE- bearing fluorite deposits

Keban (KB): This deposit is located at Keban, in east-central Anatolia (Fig. 1). The geology of the region comprises Permian – Triassic metamorphic rocks and Cretaceous to Palaeocene alkaline intrusives (Şaşmaz and Çelebi, 1999; Kalender, 2011; Bünyamin, 2015). The Keban (KB) fluorite deposit is part of a metallogenic province consisting largely of Late Cretaceous carbonate-hosted skarn and replacement Pb-Zn mineralisation, and Au-Ag-Pt porphyry deposits (Yigit, 2009). The region includes several fluorite deposits, hosted both in the porphyry stocks and in the metamorphic units (Fig. 2e). The deposit described here occurs in Palaeozoic dolomitic marble and calc-schist adjacent to an alkaline intrusion (Fig. 5a). The ore resource has been estimated as 0.034 Mt of measured, 0.053 Mt of indicated and 0.1 Mt of inferred fluorite ore (MTA, 1989). Approximately 1000 tons of ore were mined annually, and sold to the Karabük Iron and Steel Factory, in the 1970s. Fluorite ore occurs as a stockwork and single veins made up of overlapping lenses, parallel to host-rock schistosity, striking broadly north-south and dipping to the east. The ore zone extends for c. 30 m within the calc-schist of the Keban metamorphic succession, with individual veins being c. 10 to 30 m long and 0.1 to 0.9 m thick (Fig.5a). The ore includes fluorite, and is unusual in containing sulphides, with minor chalcopyrite, galena, sphalerite, calcite and quartz (Table 1).

Tad Deresi (TD): This deposit is located 6 km southeast of Akdağmadeni (Yozgat) in central Anatolia (Fig. 1). As at Keban, the region is dominated by Palaeozoic metasedimentary rocks intruded by Upper Cretaceous alkaline granitoids (Şaşmaz et al., 2005a), although granitoids are not exposed in the immediate area around Tad Deresi. The fluorite-bearing ore zone occurs within Palaeozoic recrystallized limestone and at the contact between the recrystallized limestone and schists (Fig. 2f). The ore zone takes the form of E-W trending fluorite veins up to 15 cm thick emplaced into fault zones, together with associated sulphide-rich veins (Şaşmaz et al., 2005a). The ore zone is up to 1 m wide and approximately 60 m in lateral extent. Coarse-grained fluorite also occurs disseminated within the recrystallized limestone (Fig. 5b). The ore zone veins contain colourless-transparent and purple fluorite together with barite, and quartz, calcite and dolomite as gangue (Table 1). The deposit has been defined as a low temperature hydrothermal vein type by Uçurum et al., (1997) and Şaşmaz et al., (2005a).

Pöhrenk (PO): The Pöhrenk fluorite deposit is located north of Pöhrenk in central Anatolia (Fig. 1) and is hosted by Cenozoic sedimentary rocks of the Çiçekdağı basin (Genç, 2006). Fluorite mineralization occurs within Eocene limestones and an overlying Miocene sedimentary succession consisting of marl and sandstone (Fig. 2g). The distribution of ores is considered to be controlled by the basal Miocene unconformity, and the ores are largely found as breccia cements, cavity fillings and replacement ores (Genç, 2006). The ore comprises largely fluorite, barite and galena, and the fluorites are transparent to yellow and greyish (Fig. 5e) in outcrop. Approximately 0.2 Mt of ore was mined from this deposit before 2015. The deposit is defined as an interstratal karst-type formation by Genç, (2006), with the ore-forming fluids being formation waters from within the sedimentary basin.

Tavşanlı (TAV): The Tavşanlı (Kütahya) deposit is located in western Anatolia (Fig. 1). The fluorite deposit forms E-W trending veins that are emplaced into a fault zone in limestone (Fig. 2h) This Upper Cretaceous limestone represents the mega-blocks of an ophiolitic melange, formed on subducting Neotethyan oceanic crust, which has undergone blueschist facies metamorphism (Okay, 2011). The ophiolitic melange is overlain by Eocene limestone and cut by Oligocene-aged granitoids (Okay, 2011). The overlying volcano sedimentary Miocene series includes the world class Emet borate deposit.

The fluorite-bearing ore zone extends for approximately 500 m. Roughly E-W trending fluorite veins up to 50m in length occur discontinuously within this zone. They include transparent, purple and green fluorite with calcite and barite (Fig. 5f). 0.027 Mt of indicated fluorite resource was estimated by MTA (1979). Özgenç (1993b) suggested that the deposit is associated with Cenozoic magmatism that occurs in the area, with homogenization temperatures of fluid inclusions in fluorite around 270- 243 °C.

Akkaya (AK): The fluorite deposit at Akkaya is located approximately 8 km south of Feke (Adana) in southern Turkey, and occurs as a NW-trending, steeply dipping vein in Cambrian limestone (Table 1, Fig. 2i). The vein varies between 0.5 m and 2 m thick, and extends for 70 m (Fig. 5c). The ore vein includes mainly white fluorite and rarely light blue and purple fluorite, accompanied by barite and rare quartz. The Palaeozoic carbonates in the region also include barite deposits (e.g. Tordere and Tortulu Barite deposits, Taş, 2009). Özüş and Yaman, (1986) suggest that the fluorite deposit formed from formation waters, not magmatogenic water, based on the REE pattern of fluorites.

Yeşilyurt (YES): This deposit is located approximately 20 km southeast of Yeşilyurt (Malatya) settlement (Fig. 1). The fluorite deposit formed at the contact between Carboniferous limestone and overlying Permian schists (Fig. 2j). The contact has been described as an unconformity by Revan and Genç (2003), and as a thrust zone by Şaşmaz et al., (2005b). This contact zone extends for more than 20 km and is marked by brecciation with open space filling and replacement type fluorite deposits; it is thus considered here as a thrust zone. Fluorite occurs as the cement of the tectonic breccia and as massive replacement bodies. It includes mainly dark blue and dark purple fluorites (Fig. 5d) with calcite, dolomite and quartz (Table 1). This is a unique fluorite deposit because it also contains gold (Revan and Genç 2003).

5. Geochemistry

Of the analysed samples 16 are from the two carbonatite-hosted deposits, 50 samples come from the 5 deposits associated with alkaline magmatism, and 57 samples are from the 6 carbonate- hosted type deposits. While the AKC, CA and AK samples are nearly pure fluorite, the other samples are fluorite-rich ore which also contains quartz, calcite, barite, and bastnäsite. The main ore mineralogy for each deposit is shown in Table 1 and average geochemical data in Table 2. The complete geochemical dataset is presented in Supplementary Table 1.

5.1. Major and trace elements

5.1.1. Carbonatite-hosted deposits

Pure fluorite is CaF_2 and thus CaO and F contents are expected to dominate the analyses. Notably, SiO2, Fe_2O_3, and MnO contents of fluorite-rich ore samples from carbonatite-hosted deposits are also considerable (Table 2). The SiO_2 and CaO contents of the Kuluncak deposit (KUL) are higher than in Kızılcaören (KO), but the Fe_2O_3 and MnO contents are lower (Table 2). The relatively high SiO_2 content of KUL (6.12 wt%) is consistent with the presence of quartz and other silicate minerals within the ore samples (Table 1). Fe_2O_3 (4.23 wt. %) and MnO (0.44 wt. %) content of fluorite-rich samples from KO are higher than the KUL deposit (1.7 wt. % Fe; 0.17 wt. % Mn). This is related to extensive Fe and Mn-hydroxide occurrences in the carbonatite complex that developed under supergene conditions, as primary minerals such as pyrite and manganese carbonate were oxidised (Nikiforov et al., 2014). The mean LOI value (8.55 wt. %) of KUL samples is twice as high as the samples from KO (4.46 wt. %; Table 2), related to the presence of calcite in the ore paragenesis (Table 1).

The carbonatite-associated deposits are characterised by relative enrichment of REE, Nb, Be, Sr, Pb-Zn, and Th and general depletion of Se when compared with the carbonate and alkali intrusive hosted deposits (Table 2, Fig 6-8). Nb could be associated with pyrochlore and Nb- rutile, whereas REE are likely to be focused in bastnäsite.

5.1.2. Alkaline intrusive-hosted deposits

SiO_2, Al_2O_3, Fe_2O_3, and CaO contents of the alkaline-hosted fluorite ores show significant variation between deposits (Table 2). The CaO content of alkaline intrusive-hosted ores (BY, IH, AKC, CA and DIV) varies between 45 wt. % and 65 wt. % with the highest mean content of 64.75 wt. % at BY (Table 2). The highest mean SiO_2 content (21.5 wt. %) is for the ore from IH, which comprises quartz interbanded with fluorite. The mean SiO_2 contents of the ores from BY, DIV, AKC, and CA are fairly consistent, varying from 11 wt. % to 16 wt. %, and reflecting the amounts of quartz in the different deposits. The mean Al2O3 content of IH and CA is 2- 3 wt. %, indicating the presence of sheet silicates in some samples, whereas BY, AKC and DIV are less than 1 wt. %. The mean Fe_2O_3 content of the fluorite-rich DIV samples is higher than the other deposits (BY, IH, AKC and CA), due to the presence of iron-bearing minerals such as pyrite, arsenopyrite, chalcopyrite, and sphalerite within the ore paragenesis. The range of F in these deposits is between 18 wt. % and 26 wt. %, with the highest content for the near-pure fluorite ore from AKC (Table 2). The mean LOI value of CA is notably higher (11 wt. %) than the other deposits (less than 5.6 wt. %, Table 2) owing to the presence of significant amounts of calcite in some samples (Table 1).

Ba contents of the AKC, CA and IH deposits show significant variation (Table 2), having mean values of 1850, 416, and 155 ppm, respectively, which reflect a wide range in Ba contents in individual samples (e.g. 21 to 12774 ppm at AKC; Supp. Table 1). The high Ba content of some ore samples is related to variable amounts of barite in the paragenesis. The uranium content of AKC fluorite and fluorite-rich DIV samples (259 and 116 ppm, respectively), is higher than other deposits. This may be related to the U-rich nature of the host alkaline intrusive. DIV ore samples have relatively higher contents of Cu, Sn, As, Sb, Pb, Zn, Bi, Au, Ag, Co, and Ni than the other alkaline intrusive-hosted deposits (Table 1). This polymetallic composition is consistent with the mineral paragenesis consisting of pyrite, bismuthinite, sphalerite, galena, chalcopyrite, arsenopyrite and tetrahedrite (Table 1).

5.1.3. Carbonate-hosted deposits

The Yeşilyurt fluorite ore shows the highest mean SiO_2 content among these deposits (62 wt. %) owing to the presence of abundant quartz within the ore. Mean Al_2O_3 contents of the YES and KB deposits are higher (3.8 and 2.1 wt% respectively) than other deposits of this type. While the mean CaO values of carbonate-hosted deposits vary between 21 wt.% and 68 wt.%, reflecting variability of both calcite and fluorite, the F values vary between 10 wt. % and 26 wt.% and are representative of fluorite only (Table 2). Variable LOI values between 1 wt. % to 28 wt. %, can be related to the presence of calcite and clay in some ore samples (Table 2). All deposits of this type show significant Ba variations (mean Ba varies from 595 to 16434 ppm), which is consistent with variation in the amount of barite in the ore. The KB deposit has very high mean Mo, Cu, Pb, Zn, Ni, As, and Bi contents, consistent with the presence of abundant sulphides in the ore. High Pb, Zn, Ni, As, Au, and V also characterise the YES deposit (Table 2). TD fluorite ore has high Co values (mean 13 ppm), and the TAV deposit contains significant Sb (mean 178 ppm).

5.2. Rare earth elements (REEs)

5.2.1. Carbonatite-hosted deposits

The carbonatite-hosted KO and KUL deposits are recognised as potentially economic REE deposits (Goodenough et al., 2016). The analysed samples from both deposits were fluorite-rich samples, also including the REE-bearing minerals bastnäsite and britholite. Therefore, the REE contents of these samples do not directly reflect the REE content of fluorite minerals, but are representative of the overall ore. The samples from the KO deposit have very high mean ΣREE content (29982 ppm) whereas the KUL deposit has a mean of 7255 ppm ΣREE (Table 2).

The chondrite-normalized REE patterns of the KO and KUL deposits are both LREE-enriched, (Fig. 6a) with small negative Eu anomalies (mean Eu/Eu* = 0.59 for KUL (n=6) and 0.66 for KO (n=10). *(Eu / Eu* ratio where Eu* defined by $\sqrt{(SmN \times GdN)}$ formula)*). These Eu anomalies could indicate separation of the hydrothermal fluids from a magma that had fractionated plagioclase.

5.2.2. Alkaline intrusive-hosted deposits

Total LREE (La –Eu) and HREE (Gd-Lu) content of these deposits varies between 1235 and 50 ppm, and 827 ppm to 54 ppm, respectively. Among deposits of this type, the DIV deposit shows the highest REE contents, with mean ΣREE of 1363 ppm, whereas all the other ores have ΣREE < 200ppm (Table 2).

The DIV ore has a mildly LREE-enriched pattern with a moderately strong Eu anomaly (mean Eu/Eu* 0.43). This distinctive negative Eu anomaly may be associated with preference of Eu for the liquid phase (as $Eu2^{+}$) at reducing conditions during the crystallization of fluorite and coeval sulphides, or may indicate separation of the hydrothermal fluids from a magma that had fractionated plagioclase.

The other alkaline intrusive-hosted deposits do not show significant differences, having relatively flat REE patterns (Fig. 6b). Eu anomalies are weak to absent (average Eu/Eu* is 0.78 for IH samples (n=9), and > 0.85 for all other deposits of this type).

5.2.3. Carbonate-hosted deposits

Except for the Keban deposit (mean ΣREE 541 ppm), carbonate-hosted deposits generally show low total REE (Table 2).

Despite significant variations in absolute REE contents, the REE patterns of the KB, YES, TD and AK fluorites are similar, with moderate LREE enrichment, negative Eu anomalies, and flat middle to heavy REE patterns (Fig. 6c). The TAV and PO ores show a remarkably different, flat REE pattern which may appear convex through the middle REE (TAV) or show a small positive Dy anomaly (PO) (Fig. 6c). These patterns are more similar to some of the alkaline-intrusive hosted (BAY and AKC) deposits.

5.2.4. Overview of REE geochemistry

The chondrite-normalized rare-earth element patterns of these three deposit groups show significant variation. On the basis of the pattern shape, four different types of REE patterns can be defined from the 13 fluorite- REE deposits.

The first type of pattern is characterized by a high total REE content and a strong LREE enrichment, with steep REE trends. The KO, KUL, KB and YES deposits are typical examples of this pattern type, which is very similar to that of other carbonatite-alkaline complex-hosted REE-fluorite deposits in the world, like the Bayan Obo deposit (Xu et al. 2008), or the Gallinas Mountains Fluorite±REE deposit (Fig. 6a, b).

The second type of REE pattern is characterized by a moderate REE content and flat to gently LREE-enriched patterns. The BY, IH, CA, PO and TD deposits, which all cluster in the same region close to the large Bayındır pluton, are examples of this type. The fluorine in these fluorite deposits could have originated from a common source, possibly associated with a post-magmatic hydrothermal system, and been deposited both in the magmatic body and in the country rock. Relatively flat REE patterns are commonly found in alkaline silicate igneous intrusions (Goodenough et al., 2018).

The third type of REE pattern, shown by the DIV and the AK fluorite deposits, is characterized by strong negative Eu and positive Y anomalies, with a gently sloping pattern from LREE to HREE. Despite having such different REE abundances, the patterns are so similar that similar processes are likely to have controlled their formation. The strong negative Eu anomaly may indicate reducing conditions during the transportation and deposition of the fluorite; this is consistent with the presence of sulphides in the DIV deposit.

The fourth- type of pattern is characterized by the MREE and HREE enrichment of the carbonate-hosted TAV deposit, which shows a saddle shape, with no signs of Eu depletion or Y increase.

6. Fluid Inclusion Studies

6.1.Fluid inclusion petrography and typology

Primary and secondary fluid inclusions were distinguished according to the criteria described by Roedder (1984) and Van den Kerkhof and Hein (2001). Microthermometric measurements were carried out on Fluid Inclusion Assemblages (FIAs) of the primary types of fluid inclusions hosted by fluorite minerals. All fluorite samples except those from the AK and YES deposits include measurable inclusions. Inclusion size varies between 10 and 30 µm and rarely exceeds 150 µm. Two different types of fluid inclusions are identified in the studied samples at room temperature. These are; (i) aqueous liquid-vapour-solid/multisolid (LVS-type) inclusions and (ii) aqueous liquid- vapour (LV-type) inclusions (Fig. 7).

Among the deposits, the KO, KUL, DIV and KB fluorites include LVS and LV-type, and the BY, IH AKC, TAV, and PO fluorites include LV type inclusions (Fig. 7). Except for a few inclusions in PO samples, the homogenization occurred in the liquid phase. In LVS type inclusions, we could not determine the composition of the solids except for halite and sylvite.

To avoid stretching and decrepitation of the inclusions (mostly in LVS-type), cooling measurements to determine the low-temperature phase transitions were performed before T_h measurements. The salinity of LV-type inclusions has been calculated from Tm-ice using the equation of Roedder (1984) and the PC program evaluated by Bakker (2003). For LVS-type inclusions, salinity of inclusions was calculated from halite and sylvite melting temperatures. The last ice melting of some inclusions occurred at higher temperatures than 0°C. The salinity of this kind of inclusion was estimated from clathrate melting temperature using the equation reported by Darling (1991). Most of the solid phases in LVS-type inclusions did not melt, so that the salinity of these inclusions could not be calculated.

6.2.Carbonatite -hosted deposits

KO and KUL fluorites include LVS and LV-type inclusions at room temperature. The size of fluid inclusions varies between 10 and 40 µm for KO, and between 15 and 50 µm for KUL. Neither deposit's fluid inclusions contain carbonic phases at room temperature, but melting of clathrate above 0 °C indicates that they should contain carbonic phases such as CO_2 or CH_4. The ranges of T_e values of LVS and LV-type inclusions are between -84 and -41°C, and -83 and -38 for KO, and between -97 and -41°C, -94 and -53 °C for KUL, respectively (Table 3; Fig. 8a). Clathrate formation occurred in most of the LVS and LV-type inclusions of KO and KUL. The clathrate melting of KO samples occurred over a very wide interval (+8 and +20 °C for LVS type, and +7 and +24°C for LV-type). In KO samples the clathrate melting temperature for KUL varies between +3°C and +22°C, and between +5 and +10 °C for LVS and LV-type inclusions, respectively. The salinity of KO and KUL is approximately 32.2 wt. % NaCl eq. and 64 wt. % NaCl eq. for LVS, and approximately 10.85 wt. % NaCl eq. and 4.3 wt. % NaCl eq. for LV-type inclusions, respectively (Fig. 9d). There are large differences between the T_h values of both deposits: 212-293 °C for LVS-type, 150-394°C for LV-type of KO, and >580°C for LVS-type, and 145-600°C for LV-type of KUL (Fig. 9a).

6.3.Intrusive-hosted deposits

DIV fluorites include LVS and LV-type inclusions. Primary and pseudo-secondary inclusions were measured. Microthermometric data varies between -69.5 °C and -24 °C for T_e, -14 °C and -8 °C for Tm-ice, and +1 and +6.1 °C for $T_{m\text{-}clth}$, respectively (Table 2; Fig. 8b). The T_h and salinity values of DIV samples vary between 190 - 455 °C, and 10 - 32 wt. % NaCl equivalent, respectively (Table 3; Fig. 9b).

The BY, IH, CA and AK fluorites include LV-type inclusions. The T_e values of BY, IH, CA and AKC vary between -69 and -38 °C, -80 and -68 °C, -83 and -30 °C, -63 and -47, respectively. The $T_{m\text{-}ice}$ values of these deposits vary between -10 and -1.8 °C, -5.1 and -3 °C, -4.9 and -4.3 °C, -5 and -2 °C, respectively. Even though there is no carbonic phase at room temperature, an inclusion of Cangıllı fluorite includes CO_2, recognisable due to clathrate melting at +3.5 °C (Table 3). The homogenization temperature (T_h) of intrusive-hosted deposits varies between 127 and 456 °C being 184-397 °C for BY, 165-385°C for IH, 127-456 °C for CA, and 208-280 °C for AKC (Fig. 9b). The salinity of intrusive-hosted deposits varies between 1 and 13 wt. % NaCl equivalent as being 1.7-12.9 wt. % for BY, 5.1-8.3 for IH, 6.5-11.2 for CA and 3.5-7.9 for AKC (Fig. 9e).

6.4.Carbonate-hosted deposits

Among the carbonate-hosted deposits, suitable fluid inclusions for microthermometric study have been detected from KB, TD, and PO deposits.

KB fluorites include LVS and LV-type inclusions. Solid phases of the LVS-type have been identified as halite and sylvite according to their optical properties. The T_e values of KB vary between -75 and -39°C, and -65 and -44°C for LVS and LV-type, respectively. The salinity of LVS and LV-type inclusions varies from 48 to 61 wt. %NaCl equivalent, and from 7 to 19 wt.% NaCl equivalent, respectively. Even though it was not detected at room temperature, a few inclusions of LVS-type, and one inclusion of LV-type, contain carbonic phases which are indicated by melting of clathrate between +6.9°C and 13°C, and at 5.8°C, respectively (Table 1). The range of homogenization temperature of LVS-type inclusions varies between 425 °C and 600°C. Several LVS-type inclusions did not homogenize at 600°C indicating higher T_h values or stretching phenomena. On the other hand, LV-type inclusions show T_h values as 123-510°C. The homogenization of LV and LVS-type inclusions occurred in the liquid phase (Fig. 9c).

PO, TD and TAV fluorites include LV-type inclusions at room temperature. The T_e values of LV-type inclusions vary between -67.5 °C and -40.5°C, between -83.7 °C and -39°C, between -71.5°C and -47.7°C for PO, TD and TAV, respectively (Fig.10c). The $T_{m\text{-}ice}$ and salinity values of these deposits vary from -1.1 to -7.9°C, and 3.7 wt. % and 10.24 wt. % NaCl equivalent for PO, as -16°C and -1.2°C, and 1.7 and 19.6 wt. %NaCl equivalent for TD, as -0.5 and -4.2 °C, and as 1 and 12 wt.% NaCl equivalent for TAV (Fig. 9f). The T_h values of PO, TD and TAV vary between 150 °C and 471°C, 165 °C and 414°C, 190 and 400°C, respectively (Table 3).

6.5.Solution systems and T_h (°C) versus salinity (wt. % NaCl equivalent)

Although the majority of T_e values of the carbonatite-hosted KUL deposit plot between -56 and -40 °C for LVS-type inclusions, and -88 and -78 °C for LV-type inclusions (Fig. 8a.), the T_e values of the KO deposit show a wide range. A carbonic phase was not detected at room temperature, but a prominent feature of both KUL and KO deposits is formation of clathrate during freezing of inclusions, which indicates carbonic phases in the solution system. Although melting of clathrate occurred between 0 and 10 °C for the KUL deposit, in the KO deposit it generally occurred above 10°C. The melting behaviour of clathrate indicates that fluids responsible for formation of the KUL deposit include CO_2 as the dominant carbonic phase, while the KO deposit includes CH_4 in addition to CO_2 (Van den Kerkhof and Hein, 2001, and references therein).

The T_e values of fluid inclusions belonging to intrusive-hosted deposits vary between -84°C and -24 °C (Fig. 8b). Among the intrusive-hosted deposits, Te values of IH, CA and AKC vary between -80 and -68 °C, -54 and -46 °C, and -56 and -48 °C, respectively (Fig. 8b). While the T_e values of fluid inclusions from IH indicate LiCl-bearing fluids, the T_e values of CA and AKC indicate $CaCl_2$-dominated fluids. The clathrate formation during the freezing of LVS and LV-type inclusions of the DIV deposit is contrasts significantly with other deposits in the intrusive-hosted group. The presence of clathrate indicates that the fluid responsible for the formation of DIV fluorite contained a carbonic phase such as CO_2 (Van den and Thiery, 2001).

There is no significant interval that distinguishes carbonate-hosted deposits in respect to T_e values, because the T_e values of carbonate-hosted deposits vary between -79°C and -38 °C without concentration in a narrow range (Fig. 8c). Such a wide variety of T_e values may indicate that fluids responsible for the formation of fluorite were not homogenised and contained different cations in addition to Na^{+}, such as K^{+}, Mg^{+}, Ca^{+2}, and probably Li^{+} (Shepherd et al., 1985). The KB fluorite clearly differs from other carbonate-hosted deposits by formation of clathrate (Fig. 8c). Clathrate formation at low temperature indicates that the fluids responsible for formation of the KB fluorites contained a significant carbonic phase, and the melting of the majority of clathrate between 0 and 10°C shows that CO_2 was the carbonic phase (e.g. Van den Kerkhof and Hein, 2001). Two clathrates melted at a higher temperature than 10°C which may indicate possible carbonic phases such as CH_4 apart from CO_2.

The T_h intervals vary between 200 and 600 °C for carbonatite-hosted deposits (Fig. 9a), 150 and 400 °C for intrusive-hosted deposits (Fig. 9b), and 150 and 450 °C for carbonate-hosted deposits (Fig. 9c). T_h values of the KUL deposit are largely between 350 and 600 °C, but, with the exception of T_h of one LV and one LVS-type inclusion, the KO deposit's T_h varies between 200 and 400 °C. The T_h values of the measured fluid inclusions in fluorite may be considerably higher than the true homogenization temperatures due to overheating of the inclusions (Bodnar and Bethke, 1984).

The T_h vs. wt. % NaCl diagram shows that the fluids responsible for formation of carbonatite-associated deposits have higher temperature and salinity than intrusive and carbonate-hosted deposits (Fig. 9 d,e,f). Even though the KB fluorites formed within a sedimentary host, their fluid inclusion features (such as inclusion types, T_h and salinity) resemble those of the carbonatite-hosted fluorite deposits, KO and KUL (Fig. 9a and c). These features indicate that KB fluorites could be related to fluids derived from a carbonatite magma. The fluids related to carbonatite complexes are oversaturated, represented by daughter minerals in fluid inclusions.

7. Discussion

7.1 Geological environment of formation

The Kızılcaören F- REE deposit contains nearly horizontal lenses of banded ore, whereas the majority of the other deposits described here comprise steeply dipping veins. The largest banded ore body in the Kızılcaören district shows a stratification from fluorite-rich banded ore at the base, through more carbonate-rich banded ore in the middle, to Mn oxide-rich weathered ore at the top. Formation of such a chemical stratigraphy, which is laterally extensive, indicates repetitive injection of substantial amounts of Ba, Ca, Mn, and F rich fluids over a period of time

Field relationships are consistent with formation of the banded ore at Kızılcaören by repeated injection of carbonate-rich saline fluids into the host rock and trapping of these fluids at particular horizons, where they cooled to form the banded ore. These fluids are considered most likely to have formed by liquid immiscibility from the carbonatite magmas that also have been recognized in the deposit (Nikiforov et al., 2014). The vertical ore veins that occur in the deposit appear to represent the feeder system of the ore lenses. The banded ores of Kızılcaören show clear similarities to the banded ores of the Bayan Obo deposit in China, which are considered to have formed from several phases of metasomatism by hydrothermal fluids (Smith et al., 2015). At Kızılcaören, there is evidence for initial silica-rich hydrothermal fluids, causing silicification, which then created a trap for repeated episodes of hydrothermal fluid injection, leading to the formation of banded ore bodies.

In contrast to Kızılcaören, the other deposits described here represent more typical vein-type fluorite deposits.

7.2 Geochemical environment of formation

The Kızılcaören deposit is the most REE-enriched of all the F-REE deposits described here and is also strongly enriched in Nb, Th, Sr and Ba. The characteristic geochemical features of this deposit, including strong LREE enrichment and a weak negative Eu anomaly, are shared by the KUL, KB and YES deposits. The REE patterns of this group are similar to those of other alkaline and carbonatite- hosted REE-fluorite deposits, such as the Bayan Obo deposit (Zhongxin et al., 1992, Yang et al., 2003, Yang et al., 2009, Lai et al., 2012) and the Gallinas Mountains deposit (Willams-Jones et al., 2000). Mineralogically, all these ores contain sulphides within the paragenesis; fluorite-barite-bastnäsite mineralization with pyrite is a typical feature of mineralization associated with alkaline and carbonatite magmatism in areas such as the Chinese Mianning-Dechang REE belt (Hou et al., 2009). In contrast, the flatter REE patterns of most of the alkaline-intrusive hosted deposits are consistent with fluorites associated with other alkaline intrusive complexes such as those of the Gardar Province in Greenland (Schonenberger et al., 2008). The TREE contents of the Turkish F-REE deposits increase with increasing salinity and formation temperature which is in good agreement with experimental solubility studies on REE (Migdisov and Williams-Jones, 2008, Williams-Jones et al 2012). Williams -Jones et al. (2012) stated that LREE complexes are typically more stable than HREE complexes in hydrothermal fluids. In other words, LREE can be mobilized in a wide range of hydrothermal conditions whereas the HREE are more commonly immobile. These authors described the remobilization of LREE from the magmatic - type Nechalacho and Strange Lake REE deposits, which occur in layered alkaline complexes in Canada.

According to Tsay et al. (2014) LREE/HREE fractionation may occur in the presence of chloride ligands at high temperature and each type of ligand (Cl^{-}, F^{-}, CO_3^{-2}, SO_4^{-2}) leaves a characteristic REE pattern, reflecting the preferences of REE complexation. The LREE enrichment at the higher temperature deposits, (Kızılcaören, Kuluncak, Keban and Divriği) could be related to the dominance of Cl as a ligand in the hydrothermal fluids, leading to preferential remobilization of the LREE. In contrast, the middle and heavy rare earth elements may have been preferentially carried as fluoride complexes. The LREE-rich hydrothermal fluids derived from carbonatites deposited bastnäsite, fluorite and apatite in relatively high-temperature hydrothermal deposits. In other deposits, sourced from alkaline magmatic and other hydrothermal fluids, REE concentrations are lower and primarily associated with fluorite, and REE patterns are flatter.

The F-REE deposits of Turkey show a good positive correlation between Nb + Ta and TREE (Fig. 10), which can be used for discrimination of the deposits that formed in association with different magmatic types. The KO and KUL deposits (characterized by high Nb) stand out on this figure as being distinctive from all the other deposits described here. Nb is typically enriched in carbonatites, associated with pyrochlore and other Nb-bearing minerals. As well as Nb, Ta enrichment is also typical for the carbonatite hosted

F-REE deposits, and likely to indicate an enriched mantle source. On the other hand, Se is typically enriched by low temperature hydrothermal processes (Dill, 2010), and shows relative enrichment from the high temperature carbonatite - associated fluorite deposit to moderate-temperature intrusive-hosted deposits. The highest Se contents occur in association with the lowest temperature carbonate hosted fluorite deposits. Our proposed Nb+Ta vs TREE diagram seems to differentiate high temperature carbonatite-related deposits from lower-temperature deposits.

Many authors use a classification of the fluorite deposits as pegmatitic-hydrothermal or sedimentary according to their Tb/La and Tb/Ca content (Schneider et al., 1975; Möller et al., 1976; Möller and Morteani, 1983). Owing to relatively low stability of LREE complexes, the earlier phase fluorites are enriched in La, and poor in the HREE such as Tb (low Tb / La ratio). With the progress of crystallization related to degradation of the LREE-fluorine complex, fluids can become enriched in HREE and this stage of fluorite is characterized by high Tb/La ratios.

On Tb/Ca and Tb/La variation diagrams, the carbonatite-hosted fluorites (KO and KUL), some alkaline intrusive-hosted deposits (DIV), and carbonate-hosted (KB) locate in the 'pegmatitic' area whereas low-temperature carbonate hosted and some intrusive hosted deposits mostly locate in the hydrothermal fields (Fig. 11). Whilst these diagrams do not clearly indicate fluorite ore associated with carbonatites, the 'pegmatitic' field discriminates ores with high total REE with LREE enriched over HREE; these are characteristic features of carbonatites. In general, these discrimination diagrams also indicate that the DIV and KB deposits show similarity to the carbonatite hosted KO and KUL deposit (Fig. 11). The KB and DIV ores are characterized by high REE contents, high formation temperature and high fluid salinity, high Nb, Be and low Se contents relative to low temperature deposits. Thus, although the KB and DIV complexes are not known to be associated with carbonatites, it seems possible that carbonatites remain to be found in these areas.

The ore in these deposits typically contains quartz and has moderately high SiO_2 contents, possibly indicating long-term fluid flow in silicic basement rocks and deposition at low temperature shallow level conditions. The YES deposit shows a very similar pattern shape to those of the REE- rich first group of deposits, but has low REE content. It is likely that all these deposits were associated with a late magmatic hydrothermal system, and were deposited in either the magmatic body or its country rocks. However, the significantly lower REE contents, higher SiO_2 contents, and low temperature/ salinity of the fluids, all suggest the introduction of a second fluid component which was not derived from the carbonatite magmatic system.

The second type of deposit is hosted by alkaline intrusives and includes the BY, IH, CA, PO and TD deposits. The relatively flat REE patterns of these deposits are consistent with their formation in association with an alkaline magmatic system.

The third type of deposits are the carbonate -hosted TAV and AK deposits which display very low total REE, very low amounts of trace elements, and have low temperature - low salinity fluid or lack any fluid inclusions (AK). The sources for these deposits are more likely to be basinal brines, with very little contribution from the magmatic system.

As a unique case, the Akkaya fluorite deposit has no fluid inclusions and very low REE, and locates in very different areas in discrimination diagrams (Fig. 6c) from the other carbonate-hosted deposits. The source of hydrothermal fluids for this deposit is uncertain.

7.3 Mineralizing fluids and the physical-chemical regime

As a general rule, the REE contents of the fluorite deposits of Turkey increase with increasing formation temperature and salinity.

A high homogenization temperature between 400 to 600 °C, high salinity (45 % < NaCl eq < 65 wt. %), presence of CO_2 and CH_4 carbonic phases and solid – bearing inclusions (LVS) are common fluid inclusion features (Table 3) of the first group, including the KO, KU, DIV and KB deposits. The homogenization temperature of the Kızılcaören REEs+ fluorite deposit ranges between 200 and 600 °C. This wide spectrum of ore-forming fluid temperatures could be related to multi-phase hydrothermal processes related to an alkaline-carbonatite magmatic system or there may also be data belonging to petrographically undifferentiated secondary inclusions.

The second group of deposits largely comprises the alkaline-intrusive hosted deposits and is characterized by moderate total REE, nearly flat REE trends, low temperature and low salinity fluids. As well as the alkaline-intrusive hosted Bayındır, Akçakent, İsahocalı, and Cangıllı deposits, the carbonate-hosted Pöhrenk, Yeşilyurt and Tad Deresi deposits appear to be part of this group, which only occurs in the Central Anatolian metamorphic massif. Fluid inclusions of this group of deposits are characterized by relatively low to moderate temperature homogenization (150 and 450°C), moderate to low salinity (2-12 wt. % NaCl) and LV-type inclusions. Carbonic species are not found in the fluid inclusions of this group of deposits.

Homogenization temperature (aver. Th>300°C) and salinity (aver. 10 % wt. NaCl equiv.) of the fluids in fluorite minerals of the carbonate-hosted deposits of Turkey do not resemble MVT deposits which have approximately 175°C Th and 25±5 % wt. NaCl equivalent salinity (Bodnar et. al. 2014).

Fluid inclusion characteristics of the carbonatite-hosted Kızlcaören and Kuluncak F-REE deposits are somewhat different to the Bayan Obo deposit, where it has been shown that the bastnäsite formed between 240°C and 340°C, and fluorite between 150°C to 240°C, from fluids containing 1 to 7 % wt. NaCl equivalent for bastnasite and 1% to 60% wt. NaCl equivalent for primary fluorite (Smith and Henderson 2000). The Gallinas Mt. REE-F deposit formed between 300°C and 400°C from fluids containing 12 to 18% wt. NaCl equivalent (Williams-Jones et al. 2012). Our results from Kızılcaören indicate generally higher formation temperatures, with mean temperature for LV type 299°C and LVS type 255°C, and salinity 5 % and 64 % wt. NaCl equivalent, respectively. The Kuluncak deposit has mean temperature for LV type >375°C and LVS type >587°C, and salinity 7% and 64 % wt. NaCl equivalent, respectively. In the light of these data two conclusions can be made; (1) Ore forming fluids of the carbonatite-hosted Turkish deposits are highly saline and appear to have formed at slightly higher temperatures relative to the Bayan Obo or Gallinas Mt deposits (2) The fluid inclusions in the minerals of the Bayan Obo and Gallinas Mt deposits may have been affected by secondary processes over time.

7.4 Redox conditions

The redox condition during the deposition of fluorite is not clear for all deposits, despite some of them containing sulphides such as pyrite. The oxidation stage of europium during the hydrothermal and metamorphic processes has been discussed by Bau (1991) and a positive Eu anomaly has been interpreted as indicating oxidizing formation conditions by some authors (Şaşmaz et al., 2005). In reduced hydrothermal fluid, Eu exists mostly as Eu^{2+} rather than the usual Eu^{3+} and if reduced conditions do not change then Eu stays as Eu^{2+} in the fluids, together with Sr^{2+} which is a similar ionic radius. These elements should behave compatibly in a fluorite lattice owing to both valence and radii similarities among

Ca^{2+}, Sr^{2+}, and Eu^{2+} (Shannon, 1976). As a result, if fluorite crystallizes under reducing conditions, Eu should show positive correlation with Sr and some Ba. To understand this phenomenon, correlation coefficients (r) between Eu, Sr, and Ba for each deposit have been defined. Highly variable correlation coefficient values (r) between Sr and Eu, varying from -0.84 (IH) to + 0. 89 (PO), indicates that fluorite may have crystallized under both reducing and oxidizing conditions. This also indicates that fluorite- REE deposition is independent from redox change at the deposition site. Variable r values indicate that the main factors for fluoride-REE precipitation from the hot fluids possibly were increasing in pH or decreasing of temperature or both. According to the strong positive correlation between Eu and Rb, Ba, Ce, Sr for the PO deposit (0.71, 0.89, 0.39, 0.89) and the negative correlation for the AK deposit (-0.50, -0.64, -0.22, -0.59) we suggest that, the PO deposit represents oxidizing formation conditions, whereas AK formed under reducing conditions (Fig.12).

7.5 Synoptical overview

REE -bearing fluorite deposits of Turkey are located in the Anatolides tectonic unit and formed from the Late Cretaceous to the Miocene time interval (Table 4). Beside the Kızılcaören F-REE-Ba-Th deposit, the other magmatic rock - hosted deposits may have formed in association with A - type magmatism after the collision between the Anatolides and Pontides. Alkaline intrusive - hosted deposits (Bayındır, İsahocalı and Akçakent deposits) show a close association with dark green lamprophyre within syenitic and monzonitic intrusive bodies, and the ore forming fluids have typically made use of the same pathways, such that fluorite is commonly associated with minor intrusions. Fluorine, REE and other elements originated from the magmatic system and were deposited either ashydrothermal vein-fillings or within the sedimentary country rocks as hydrothermal replacement and/or vein-filling mineralisation.

REE - bearing fluorite veins in the Paleozoic, Mesozoic and Cenozoic sedimentary rocks do not have a stratabound or manto- type ore geometry. They mostly occur in passive margin carbonates and lack any spatial relationship with magmatic bodies. Therefore, the carbonate - hosted Akkaya, Yeşilyurt, and Tavşanlı fluorite veins can be compared with the MVT fluorite deposits of USA, Kentucky- Illinois region (Denny et al. 2008), England, Pennines region, (Bau et al. 2003), Mexico, La Encandata (Levresse et al.,

(2006) and Spain, Austrias (Iglesias and Loredo 1994). The formation mechanism and source of fluorine for these deposits is still enigmatic and is not attributed to a magmatic activity. The REE patterns of the studied fluorite deposits were compared to the La Encantada deposit, which is the best example of the MVT fluorite deposit (Levresse et al. 2006). As shown in Fig.13, the REE patterns of the carbonate - hosted fluorite deposits of Turkey are very different to the La Encantada deposit.

The REE - rich fluorite deposits of, Central Anatolia, namely Kuluncak, Divriği and Keban, are similar to those of the Maoniuping, Dalucao and Lizhuang deposits of the Sichuan region, China, in many respects such as association with post collisional magmatism, mineralization age, host lithology, ore geometry, formation temperature and ore mineralogy. Lui et al. (2018) and Liu and Hou (2017) reported that the Maoniuping region fluorite-bearing REE deposits were associated with post collisional alkaline magmatism that formed along a crustal scale fault zone between the orogenic zone and craton. The REE– bearing fluorite deposits of Turkey are also concentrated between the İzmir Ankara Erzincan Suture zone and the crystalline basement of the Anatolides, which is similar to the geological setting of the Maoniuping region deposits. Similar to the Central Anatolian deposits, the Kızılcaören F-REE-Ba-Th deposit of western Anatolia is also located in a collision zone between the edge of the Anatolian crystalline craton and an Upper Cretaceous aged melange formation.

REE contents of the fluorite deposits show a decrease from orogenic zone to the interior of the Anatolide micro continent. These outer margin deposits occur in the passive margin carbonates and show no clear link to the magmatism; they can be classified as a fault controlled fluorite deposit according to the classification schema which made by Dill et al. (2008).

Chondrite normalized REE pattern of the Turkish F-REE deposits are compared to different types of F-REE deposits worldwide (Fig 13). REE data from the Mexican La Encantada deposits is taken as representative for MVT, from the Bayan Obo deposit for carbonatite, and from the Gallinas Mt. deposits for the alkaline magmatic deposit type.

The carbonatite-associated fluorite-REE ores of Turkey show a LREE enriched pattern which has similarities to the REE patterns of the Bayan Obo and Gallinas Mt deposits. This may be consistent with all the evidence that relates these deposits to carbonatite magmatism. The alkaline intrusive-hosted REE-bearing fluorite deposits of Turkey have much flatter REE patterns which is consistent with fluorite REE patterns from the Gardar Province (Schonenberger et al., 2008). The REE data show that the fluorite deposits of Turkey do not constitute manto-type deposits (La Encantada deposit, (Fig. 13) associated with orogenic fluid migration, in the manner of the Mexican or Alpine deposits.

According to Gagnon et al., (2003) fluorites associated with alkaline magmatism are LREE-rich, lack negative Eu anomalies, and have positive Y anomalies. Fluorites associated with granites are characterized by lower LREE content, negative Eu anomalies, and positive Y anomalies. The fluorites from Turkey show wider variability in their REE patterns, and this may indicate that the deposits formed more or less by association with carbonatite and alkaline magmatism but with a variable contribution from basinal fluids.

8.Conclusions

Carbonatite- hosted, alkaline intrusive- hosted and carbonate-hosted REE-bearing fluorite deposits of Turkey were formed in association with post-collisional alkaline-carbonatite magmatism in Cretaceous to Miocene time interval.

Carbonatite - associated F-REE deposits reveal high temperature and high salinity fluid inclusion characteristics, and LREE, Nb, Be and Th enrichment. Alkaline intrusive-hosted REE-bearing fluorite deposits typically have flatter REE patterns and relatively low homogenization temperature characteristics. Sediment-hosted, low-temperature REE-bearing fluorite deposits display low TREE, strong F - Si association, a flat chondrite -normalized REE pattern, relatively low salinity and low homogenization temperature. The REE composition and/or chondrite normalized REE patterns of the carbonatite -hosted Kızılcaören F-REE deposit have similarities to those of the Mountain Pass, USA and Bayan Obo and Maoniuping region deposits in China. The geochemical and fluid inclusions feature of the deposits can be explained by variable amounts of magmatic fluids derived from the alkaline-carbonatite system mixing with other less REE-enriched fluids.

Although Turkey has a number of E-W trending parallel magmatic belts (the Pontides, Anatolides and the Taurides), the REE-bearing fluorite mineralizations of Turkey occur only in the Anatolides. While the carbonatite-hosted Kızılcaören deposit formed related to Hellenic subduction, the other deposits were formed in association with post-collisional A-type alkaline magmatism from the Upper Cretaceous to the Oligocene.

Acknowledgements

Special thanks to Eti Maden Operations General Directorate for their permission to the field study at the Kızılcaören deposit. This work was partly supported by Scientific Research Projects Unit of Istanbul University. Project number 498/05052006”.

References

Altuncu, S., 2009. Comparative investigation of the fluorite deposits in Turkey. Unpublished Ph. D. Thesis, Istanbul University, 147 p.

Altunkaynak, S., Dilek, Y., Genç, Ş.C., Sunal, G., Gertisser, R., Furnes, H., Foland, K.A., Yang, Y., 2012a. Spatial, temporal and geochemical evolution of Oligo-Miocene granitoid magmatism in western Anatolia, Turkey. Gondwana Res. 21, 961-986

Altunkaynak, S., Sunal, G., Aldanmaz, E., Genç, S.C., Dilek, Y., Furnes, H., Foland, K.A., Yang, J., Yıldız, M., 2012b. Eocene granitic magmatism in NW Anatolia (Turkey) revisited: new implications from comparative zircon SHRIMP U-Pb and 40Ar-39Ar geochronology and isotope geochemistry on magma genesis and emplacement. Lithos, 155 289-309

Aysal, N., 2015. Mineral chemistry, crystallization conditions and geodynamic implications of the Oligo–Miocene granitoids in the Biga Peninsula, Northwest Turkey. Journal of Asian Earth Sciences, 105 68-84.

Bakker, R.J., 2003. Package FLUIDS 1. Computer programs for analysis of fluid inclusion data and for modelling bulk fluid properties. Chemical Geology, 194, 3-23

Bau, M., 1991. Rare-earth element mobility during hydrothermal and metamorphic fluid–rock interaction and the significance of the oxidation state of europium. Chem. Geol. 93, 219-230.

Bau, M., Romer, R.L. Lüders, V., Dulski, P., 2003. Tracing element sources of hydrothermal mineral deposits: REE and Y distribution and Sr-Nd-Pb isotopes in fluorite from MVT deposits in the Pennine Orefield, England. Mineralum Deposita, 38-8, 992–1008.

Bensurov, V.L., Kurrl'chrkove, G.ye., 1966. On the forms in which tin is transported in hydrothermal solutions. Geochent, Int. 3, 759-764.

Berg, Van Den F., 2017, Kızılcaören fluorite-barite-bastnäsite carbothermal ore deposits: Rare earth elements in a post-collisional setting Masters of Science Thesis, University of Exeter, 132 p.

Bodnar R.J., Bethke, P.M., 1984. Systematics of Stretching of Fluid Inclusions I: Fluorite and Sphalerite at 1 Atmosphere Confining Pressure. Economic Geology 79, 141-161.

Bodnar R.J., Lecumberri-Sanchez P., Moncada D. and Steele-MacInnis M. 2014. Fluid Inclusions in Hydrothermal Ore Deposits. In: Holland H.D. and Turekian K.K. (eds.) Treatise on Geochemistry, Second Edition, 13, 119- 142. Oxford: Elsevier.

Boynton, W. V., 1984. Geochemistry of the rare earth elements: meteorite studies. In: Henderson, P., (ED). REE Geochemistry. Elsevier, Amsterdam, 63-114

Boztuğ, D., 1998a. Post-collisional Central Anatolian alkaline plutonism, Turkey. Turkish Journal of Earth Sciences, 7, 145–165.

Boztuğ, D., 1998b. Geodynamic significance of metamorphism-magmatism synchronization and S-I-A type magmatic rock associations in Central Anatolia, Turkey. 51th Abstracts of the Geological Congress of Turkey, Ankara, 31-33.

Boztuğ, D., Harlavan, Y., Arehart, G.B., Satır, M., Avci, N., 2007. K-Ar age, whole-rock and isotope geochemistry of A-type granitoids in the Divriği-Sivas region, eastern-central Anatolia, Turkey. Lithos, 97, 193-218.

Bühn, B., Rankin, A.H., Schneider, J., Dulski, P., 2002. The nature of orthomagmatic carbonatitic fluids precipitating REE, Sr-rich fluorite: fluid inclusion evidence from the Okorusu fluorite deposit, Namibia. Chemical Geology, 186, 75-98.

Bünyamin, A., 2015. Geochemical associations between fluorite mineralization and A-type shoshonitic magmatism in the Keban-Elazıg area, East Anatolia, Turkey. Journal of African Earth Sciences, 111, 222-230.

Chakhmouradian, A.R., Wall, F., 2012. Rare earth elements: minerals, mines, magnets (and more). Elements, 8, 347-353.

Darling, S.R., 1991. An extended equation to calculate NaCl contents from final clathrate melting temperatures in H_2O-CO_2-NaCl fluid inclusions: Implications for P-T isochore location. Geochimica et Cosmochimica Acta, 55, 3869-3871.

Denny, F.B., Goldstein, A., Devera, J.A., Williams, D.A., Lasemi, Z., and Nelson, W.J., 2008. The Illinois-Kentucky Fluorite District, Hicks Dome, and Garden of the Gods in southeastern Illinois and northwestern Kentucky, in Maria, A.H., and Counts, R.C., eds., From the Cincinnati Arch to the Illinois Basin: Geological Field Excursions along the Ohio River Valley: Geological Society of America Field Guide 12, p. 11–24, doi: 10.1130/2008.fl d012(02).

Dill, H.G., Sachsenhofer, R.F., Grecula, P., Sasvári, T., Palinkaš, L.A., Borojeviæ-Soštariæ S., Strmiæ-Palinkaš S., Prochaska, W., Garuti, G., Zaccarini, F., Arbouille, D., and Schulz H.M., 2008. Fossil fuels, ore and industrial minerals. In: T. McCann (Ed.), Geology of Central Europe, Geological Society of London, Special Publication, London, 1341–1449.

Dill, H.G., 2010. The "chessboard" classification scheme of mineral deposits: Mineralogy and geology from aluminum to zirconium. Earth Science Reviews, 100,1-420.

Dill, H.G., 2015. Pegmatites and aplites: Their genetic and applied ore geology. Ore Geology Reviews 69, 417-561.

Dill, H.G., Luna, I., Nolte, N., Hansen, B. T., 2016. Chemical, isotopic and mineralogical characteristics of volcanogenic epithermal fluorite deposits on the Permo-Mesozoic foreland of the Andean volcanic arc in Patagonia (Argentina). Chemie der Erde (Geochemistry) 76, 275-297

Dingwell, D.B., Hess, K.U., 1998. Melt viscosities in the system Na-Fe-Si-O-F-Cl: Contrasting effects of F and Cl in alkaline melts. American Mineralogist, 83, 1016-1021.

Dingwell, D.B., Scarfe, C.M., Cronin, D., 1985. The effect of fluorine on viscosities in the system Na_2O-Al_2O_3-SiO_2: implications for phonolites, trachytes and rhyolites. American Mineralogist, 70, 80-87.

Edgar, A.D., Arima, M., 1985. Fluorine and chlorine contents of phlogopites crystallized from ultrapotassic rock compositions in high pressure experiments: implication for halogen reservoirs in source regions. American Mineralogist, 70, 529-536.

Elliott, H.A.L., Wall, F., Chakhmouradian, A.R., Siegfried, P.R., Dahlgren, S., Weatherley, S., Finch, A.A., Marks, M.A.W., Dowman, E., Deady, E., 2018. Fenites associated with carbonatite complexes: A review. Ore Geology Reviews 93, 38-59.

European Commission 2014. Report on critical raw materials for the EU, Report of the ad-hoc working group on defining critical raw materials. European Commission, Raw Materials Supply Group, May 2014, 41 pp. http://ec.europa.eu/growth/sectors/raw-materials/specific-interest/critical_en

Gagnon, J.E., Samson, I.M., Fryer, B.J., Williams-Jones, A.E., 2003. Compositional heterogeneity in fluorite and the genesis of fluorite deposits: insights from LA-ICP-MS analysis. The Canadian Mineralogist, 41, 365-382.

Gammons, C.H., Wood, S.A., Li, Y., 2002. Complexation of the rare earth elements with aqueous chloride at 200 °C and 300 °C and saturated water vapour pressure. Geochem. Soc. Spec. Publ. 7, 191-207.

Genç, Y., 2006. Genessis of the Neogene interstratal karst-type Pöhrenk fluorite-barite (± lead) deposit (Kırşehir, Central Anatolia, Turkey). Ore Geology Reviews, 29, 105-117.

Giordano, D., Russell, J.K., Dingwell, D.B., 2008. Viscosity of magmatic liquids: a model. Earth and Planetary Science Letters, 271, 123-134.

Goldschmidt, V.M., 1954. Geochemistry: London, Oxford University Press, 730 p.

González-Partida, E., Carrillo-Chávez, A., Grimmer, J.O.W., Pironon, J., Mutterer, J., Levresse, G., 2003. Fluorite deposits at Encantada-Buenavista, Mexico: Products of Mississippi Valley type processes. Ore Geology Reviews, 23 (3-4), 107-124.

Goodenough, K.M., Schilling, J., Jonsson, E., Kalvig, P., Charles, N., Tuduri, J., Deady, E.A., Sadeghi, M., Schiellerup, H., Müller, A., Bertrand, G., Arvanitidis, N., Eliopoulos, D.G., Shaw, R.A., Thrane, K., Keulen, N., 2016. Europe's rare earth element resource potential: An overview of REE metallogenetic provinces and their geodynamic setting. Ore Geology Reviews, 72, 838-856.

Goodenough, K.M., Wall, F., Merriman, D., 2018. The Rare Earth Elements: demand, global resources, and challenges for resourcing future generations. Natural Resources Research, 27 (2). 201-216.

Gültekin, A.H., Örgün, Y., Suner, F., 2003, Geology, mineralogy and fluid inclusion data of the Kızılcaören fluorite barite REE deposit, Eskisehir, Turkey. Journal of Asian Earth Sciences, 21, 4, 365-376.

Gürsu, S., Möller, A., Göncüoglu, M.C., Köksal, S., Demircan, H., Köksal, F.T., Kozlu, H.,Sunal, G., 2015, Neoproterozoic continental arc volcanism at the northern edge of the Arabian Plate, SE Turkey. Precambrian Research, 258, 208-233Haas, J.R., Shock, E.L., Sassani, D.C., 1995. Rare earth elements in hydrothermal systems: Estimates of standard partial molal thermodynamic properties of aqueous complexes of the rare earth elements at high pressures and temperatures. Geochimica et Cosmochimica Acta, 59, 4329-4350.

Haque, N., Hughes, A., Lim, S., Vernon, C., 2014. Rare earth elements: Overview of mining mineralogy uses sustainability and environmental impact. Resources, 3, 614–635.

Hatzl, T., 1992. Die Genese Der Karbonatit - Und Alkalivulkanit - Assoziierten FluoritBaryt-Bastnasit - Vererzung Bei Kizilcaoren (Turkei). Munchner Geol. Hefte, 271 p.

Hein, U.F., Luders, V., Dulski, P., 1990. The fluorite vein mineralization of the southern Alps: combined application of fluid inclusions and rare earth element (REE) distribution. Mineralogical Magazine, 54, 325-333.

Hess, K.U., Dingwell, D.B., Webb, S.L., 1995. The influence of excess alkalis on the viscosity of a haplogranitic melt. American Mineralogist, 80, 297-304.

Hou, Z.Q, Tian, S, Xie, Y, Yang, Z, Yuan, Z, Yin, S, Yi, L, Fei, H, Zou, T, Bai, G and Li, X. 2009. The Himalayan Mianning–Dechang REE belt associated with carbonatite–alkaline complexes, eastern Indo-Asian collision zone, SW China. Ore Geology Reviews 36, 65-89.

Iglesias, J.G, Loredo, J., 1994. Geological, geochemical and mineralogical characteristics of the Asturias fluorspar district, northern Spain. Exploration and Mining Geology 3(1):31-37.

Işık, V., Lo, C.H., Göncüoğlu, C., Demirel, S., 2008. $^{39}Ar/^{40}Ar$ ages from the Yozgat Batholith: Preliminary data on the timing of Late Cretaceous extension in the Central Anatolian Crystalline Complex, Turkey. Journal of Geology, 116(5), 510-526.

Kalender, L., 2011. Oxygen, carbon and sulphur isotope studies in the Keban Pb-Zn deposits, eastern Turkey: an approach on the origin of hydrothermal fluids. Journal of African Earth Sciences 59, 341-348.

Kaplan, H., 1977a. Rare earth element and thorium deposit of the Kızılcaören (Eskişehir-Sivrihisar). Geological Engineering 2, 29-34.

Kaplan, H., 1977b. Final report of the Eskişehir-Sivrihisar-Kızılcaören “bastnasite-barite –flourite complex ore . MTA Report no: 482, Ankara.

Kimberly, M.M., 1979. High-temperature uranium geochemistry. Uranium deposits: their- Mineralogy and Origin (M.M. Kimberley, ed.). Mineralogical Association of Canada - Short Course Handbook. 3, 101-103.

Koç, Ş., Özmen, Ö., Doğan, A.Ü., 2003. Geochemistry of fluorite mineralization in Kaman, Kırşehir, Turkey. Journal Geological Society of India, 62, 302-317.

Koç, Ş., Reçher, A., 2001. Rare earth element geochemistry and fluid inclusion study of Akçakent fluorite veins in central Anatolian massif of Turkey. The Arabian Journal for Science and Engineering, 26, 97-107.

Köksal, S., Romer, R.L., Göncüoğlu, M.C., Toksoy-Köksal, F., 2004. Timing of post-collision H-type to A-type granitic magmatism: U–Pb titanite ages from the Alpine central Anatolian granitoids Turkey. International Journal of Earth Sciences, 93, 974-989.

Kuşcu, İ., Tosdal, R.M., Gençalioğlu-Kuşcu, G., Friedman, R., 2013. Late Cretaceous to middle Eocene magmatism and metallogeny of a portion of the Southeastern Anatolian Orogenic Belt, east central Turkey. Economic Geology, 108, 641– 666.

Lai X. D., Yang X. Y., Sun W. D. 2012. Geochemical constraints on genesis of dolomite marble in the Bayan Obo REE-Nb-Fe deposit, Inner Mongolia: Implications for REE mineralization. Journal of Asian Earth Sciences 57, 90–102

Lange, R., 1994. The effect of H_2O, CO_2 and F on the density and viscosity of silicate melts. In Mineralogical Society of America Reviews in Mineralogy, 30, 331-369.

Leo, W.G., Önder, E., Kılıç, M., Avcı, M., 1978. Geology and mineral resources of Kuluncak-Sofular area (Malatya K39-a1-K39-a2 quadrangles), Turkey. U.S. Geol. Survey Bull, 1429.

Levresse, G., Gonzalez-Partida, E., Tritlla, J., Camprubí, A., Cienfuegos-Alvarado, E., Morales-Puente, P., 2003. Fluid characteristics of the world-class, carbonate-hosted Las Cuevas fluorite-deposit (San Luis Potosí, Mexico). Journal of Geochemical Exploration, 78-79, 537 -543.

Levresse, G., Tritlla, J., Villareal, J., Gonzalez-Partida, E., 2006. The “El Pilote” fluorite skarn: A crucial deposit in the understanding and interpretation of the origin and mobilization of F from northern Mexico deposits. Journal of Geochemical Exploration, 89, 205–209.

Liu, Y., Hou, Z.Q., 2017. A synthesis of mineralization styles with an integrated genetic model of carbonatite-syenite-hosted REE deposits in the Cenozoic Mianning-Dechang REE metallogenic belt, the eastern Tibetan Plateau, southwestern China. J Asian Earth Sci 137:35–79

Liu, Y., Chakhmouradian, AR., Hou, Z.Q., Song, W., Kynický, J., 2018. Development of REE mineralization in the giant Maoniuping deposit (Sichuan, China): insights from mineralogy, fluid inclusions, and trace-element geochemistry. Mineralium Deposita https://doi.org/10.1007/s00126-018-0836-y.

Migdisov, A.A. Williams-Jones, A.E. 2008. A Spectrophotometric study of Nd(III), Sm(III) and Er(III) complexation in sulfate- bearing solutions at elevated temperatures. Geoochemica et Cosmochemica Acta,725291-5303

Migdisov, A.A. Williams-Jones, A.E. 2014. Hydrothermal transport and deposition of the rare earth elements by fluorine-bearing aqueous liquids. Mineralium Deposita, 49, 987-997.

Moix, P., Beccaletto, L., Kozur, H.W., Hochard, C., Rosselet, F., Stampfli, G.M., 2008. A new classification of the Turkish terranes and sutures and its implication for the paleotectonic history of the region. Tectonophysics, 451, 7-39.

Möller, P, Parekh, P., Schneider, H.J., 1976. The Application of Tb/Ca-Tb/La Abundance Ratios to Problems Fluorspar Genesis. Mineralium Deposita, 11, 111-116.

Möller, P., Morteani, G., 1983. On the chemical fractionation of REE during the formation of Ca-minerals and its application to problems of the genesis of ore deposits. In: Augustithis S, (Ed.). The significance of trace elements in solving Petro-genetic problems. Athens, 747-791.

MTA, 1979. Fluorite Deposits of Turkey . Publ. of Mineral Research and Exploration Gen. Dir. Ankara,. Ankara, No.176,.

MTA, 1989. Fluorite deposits of Turkey: Publ. of Mineral Research and Exploration Gen. Dir. Ankara, No: 179.

Nikiforov, A.V., Öztürk, H., Altuncu, S., Lebedev, V.A., 2014. Kızılcaören Ore-bearing Complex with Carbonatites (Northwestern Anatolia, Turkey): Formation Time and Mineralogy of Rocks. Geology of Ore Deposits, 56(1), 35-60.

O’Connor, P.J., Högelsberger, H., Feely, M., Rex, D.C., 1993. Fluid inclusion studies, rare-earth element chemistry and age of hydrothermal mineralization in western Ireland- a link with continental rifting? Transection of Institution Mining and Metallurgy (Section B: Applied Earth Sciences), 102, 141–148.

Okay, A.I., 2008. Geology of Turkey: A Synopsis. Anschnitt, 21, 19-42.

Okay, I.A., 2011. Tavşanlı Zone: The Northern subducted margin of the Anatolide-Tauride Block. Mineral Res. Expl. Bullettin of Turkey, 142, 191-221.

Okay, I.A., Satır, M., 2006. Geochronology of Eocene plutonism and metamorphism in northwest Turkey: evidence for a possible magmatic arc. Geodinamica Acta 19, 5, 251–266.

Özgenç, İ., 1993a. Geology and REE geochemisty of the Kızılcaören (Sivrihisar-Eskişehir) carbothermal bastnasite -fluorite-barite deposit. Geological Bulletin of Turkey, 36, 1-11.

Özgenç, İ., 1993b. Geology and Genesis of Fluorite Deposit of Ovacık (Tavşanlı-Kütahya). Turkey. Geological Engineering 43, 5-14.

Özgenç, İ., Kibici, Y., 1994. The geology and chemical-mineralogical properties of Britholite veins of Başören village (Kuluncak-Malatya), Turkey. Geological Bulletin of Turkey 37, 77 -85.

Öztürk, H., Kasapçı, C., Cansu, Z., Hanilçi, N., 2016. Geochemical characteristics of iron ore deposits in central eastern Turkey: an approach to their genesis. International Geology Review 58, 673-1690.

Özüş, A.S., Yaman, S., 1986. Akkaya (Feke-Adana) Fluorit-Barit minealization and its genesis. Bulletin of Geological Society of Turkey 29, 35-42.

Rajabzadeh, M.A., 2007. A fluid inclusion study of a large MVT barite-fluorite deposit: Komshecheh, Central Iran. Iranian Journal of Science & Technology, Transaction A, 31, 73 -87.

Revan, M.K., Genç, Y., 2003. Malatya-Yeşilyurt altınlı fluorit cevherleşmesi: Toroslarda Paleokarst tipi bir yatak. Jeoloji Müh. Der. 27(2), 76-93.

Richardson, C.K., Holland, H.D., 1979. Fluorite deposition in hydrothermal systems. Geochimica et Cosmochimica Acta. 43 (8), 1327-1335

Roedder, E., 1984. Fluid Inclusions: Reviews in Mineralogy, v.12, Mineralogical Society of America,Washington, D.C., 646p.

Sainsbury, C.L., 1964. Association of beryllium with tin deposits rich in fluorite. Economic Geology 59, 920- 929

Sanchez, V., Vindel, E., Martin-Crespo, T., Corbella, M., Cardellach, E., Banks, D., 2009. Sources and composition of fluids associated with fluorite deposits of Asturias (N Spain). Geofluids 9, 338-355.

Şaşmaz, A. Yavuz, F., 2007. REE geochemistry and fluid-inclusion studies of fluorite deposits from the Yaylagözü area (Yıldızeli-Sivas) in Central Turkey. N. Jb. Miner. Abh. 183(2), 215-226.

Şaşmaz, A., Çelebi, H., 1999. Geochemie der fluorite von Karamagara des Lagerstatten-distriktes Keban, Elazig, Türkei. Z. Geol. Wiss. 26(3/4), 409 -420.

Şaşmaz, A., Önal, A., Sağiroğlu, A., Önal, M., Akgül, B., 2005b. Origin and nature of the mineralizing fluids of thrust zone fluorites in Çelikhan (Adıyaman, Eastern Turkey): A geochemical approach. Geochemical Journal 39, 131-139.

Şaşmaz, A., Yavuz, F., Sağıroğlu, A., Akgul, B., 2005a. Geochemical patterns of the Akdagmadeni (Yozgat, Central Turkey) fluorite deposits and implications. Journal of Asian Earth Sciences 24, 469-479.

Sato, K., Suzuki, K., Nedachi, M., Terashima, S., Margarita, D., Ryazantseva, M.D., Vrublevsky, A.A., Khanchuk, A., 2003. Fluorite Deposits at Voznesenka in the Khanka Massif, Russia: Geology and Age of Mineralization. Resource Geology 53(3), 193-211.

Schneider, H.J., Moller, P., Parekh, P.P., 1975. Rare earth element distribution in fluorites and carbonate sediments of the East-Alpine Mid-Trassic sequences in the Nördliche Kalkalpen. Mineralium Deposita 10, 330-344.

Schönenberger, J., Köhler, J., Mark, G., 2008. REE systematics of fluorides, calcite and siderite in peralkaline plutonic rocks from the Gardar Province, South Greenland. Chemical Geology, 247, 1–2, 16-35.

Sengör, A.M.C., Yılmaz, Y., 1981. Tethyan evolution of Turkey: A plate tectonic approach. Tectonophysics 75, 181-241.

Shannon, R.D., 1976. Revised effective ionic radii and systematic studies of interatomic distances in halides and chalcogenides. Acta Crystallographica 32(5), 751-767.

Shepherd, T.J., Ranbin, A.H., Alderton, D.H.M., 1985. A Pratical Guide to fluid Inclusion Studies. Blackie, Glasgow 239 p.

Smith, M.P., Campbell, L.S., Kynicky, J., 2015. A review of the world class Bayan Obo Fe-REE-Nb deposits, Inner Mongolia, China. Multistage processes and outstanding questions. Ore Geology Reviews 64, 459-476.

Smith, M.P., Henderson, P., 2000. Preliminary fluid inclusion constraints on fluid evolution in the Bayan Obo Fe-REE-Nb deposit, Inner Mongolia, China. Economic Geology 95, 1371- 1388.

Strong, D.F., Fryer, B.J., Kerrich, R., 1984. Genesis of the St Lawrence fluorspar deposits as indicated by fluid inclusion, rare earth element and isotopic data. Economic Geology 79, 1142-1158.

Stumpel, E.F., Kırıkoğlu, M.S., 1985. Fluorite-Barite-Rare Earths Deposits at Kızılcaören, Turkey. Mitt. Österr. Geol. Ges. 78, 193-200.

Taş, A., 2009. Genetical investigation of the eastern Tauride (Adana – Feke) region barite deposits. Çukurova Üniversity, Ph D. Thesis,131

Tekin, E., Varol, B., Ayan, Z., Satir, M., 2002. Epigenetic origin of celestite deposits in the Tertiary Sivas Basin: new mineralogical and geochemical evidence. Neues Jahrbuch für Mineralogie 7, 289-318.

Thomas, R., Forster, H.J., Rickers, K., Webster, J.D., 2005. Formation of extremely F-rich hydrous melt fractions and hydrothermal fluids during differentiation of highly evolved tin-granite magmas: a melt/fluid-inclusion study. Contrib. Mineral. Petrol. 148, 582–601.

Tsay A , Zajacz Z., Sanchez-Valle C., 2014, Efficient mobilization and fractionation of rare-earth elements by aqueous fluids upon slab dehydration. Earth and Planetary Science Letters 398, 101–112

Uçurum, A., Koptagel, O., Larson, L.T., 1997. Fluid inclusion study of the Tad Deresi fluorite deposits, Akdağmadeni, Central Turkey. Turkish Journal of Earth Sciences 6(1), 13-19.

Uras, Y., Yaman, S., Öner, F., 2004. REE geochemisty of the İsahocalı (Kırşehir) and e Feke (Adana) region fluorites. Geosound 44-45,124-136.

Van den Kerkhof, A.M., Hein, U.F., 2001. Fluid inclusion petrography. In: Andersen T, Frezzotti M.L, Burke E. Eds. Fluid inclusions: phase relationships - (special issue). Lithos 55, 27-47.

Van Den Kerkhof, A.M., Thiery, R., 2001. Carbonic inclusions. In: Andersen T, Frezzotti M.L, Burke E. eds. Fluid inclusions: phase relationships - (special issue). Lithos 55, 49-68.

Verplanck, P.L., Hitzman, M.W., 2016. Rare Earth and Critical Elements in Ore Deposits. Reviews in Economic Geology 18, 365 p.

Verplanck, P.L., Van Gosen, B.S., Seal, R.R., McCafferty, A.E., 2014. A deposit model for carbonatite and peralkaline intrusion-related rare earth element deposits. U.S. Geological Survey Scientific Investigations Report, 2010-5070-J, 58 p.

Voßenkaul, D., Stoltz N.B., Meyer F.M., Friedrich B., 2015. Extraction of Rare Earth Elements from Ion Adsorption Clays, European Metallurgical Conference. Proceedings of EMC, Germany, 1-11.

Weng, Z., Jowitt, S.M., Mudd, G.M., Haque, N., 2015. A Detailed Assessment of Global Rare Earth Element Resources: Opportunities and Challenges. Economic Geology 110, 1925-1952.

Willams-Jones, A.E., Samson, I.M., Olivo, G.R., 2000. The Genessis of Hydrothermal Fluorite±REE Deposits in the Gallinas Mountains, New Mexico. Economic Geology 95, 327-342.

Williams-Jones, A.E., Migdisov, A.A., Samson, I.M., 2012. Hydrothermal Mobilisation of the Rare Earth Elements-a Tale of "Ceria" and "Yttria". Elements 8, 355-360.

Xu,C., Campbell,I.H., Kynicky J, Chen Y., Huang, Z, Qi,L., 2008 Comparison of the Daluxiang and Maoniuping carbonatitic REE deposits with Bayan Obo REE deposit, China. Lithos 106, 1-2, 12-24

Xu, C., Taylor, R.N., Li, W., Kynicky, J., Chakhmouradian, A.R., Song, W., 2012. Comparison of fluorite geochemistry from REE deposits in the Panxi region and Bayan Obo, China. Journal Asian Earth Sci. 57, 76-89.

Yaman, S., 1984. Thermo optic analyse of the Bayındır (Kaman) fluorite veins. Earthsciences, Haccettepe University 11, 23-30.

Yaman, S., 1985. Geology and fluid inclusion study of the Akçakent (Çiçekdağı-Kırşehir) Region Fluorite deposits. Bulletin of Geology Society of Turkey. 22, 73-78.

Yang, X. M., Yang, X. Y., Zheng Y. F., Le Bas M. J., 2003. A rare earth element-rich carbonatite dyke at Bayan Obo, Inner Mongolia, North China. Mineralogy and Petrology 78, 93–110.

Yang, X. Y., Sun W. D., Zhang Y. X., Zheng Y. F., 2009.Geochemical constraints on the genesis of the Bayan Obo Fe-Nb-REE deposit in Inner Mongolia, China. Geochimica et Cosmochimica Acta 73, 1417–1435.

Yigit, O., 2009. Mineral Deposits of Turkey in relation to Tethyan Metallogeny: Implications for Future Mineral Exploration. Economic Geology 104, 19-51.

Yılmaz, Y., Tüysüz, O., Yiğitbaş, E., Genç, Ş.C., Şengör, A.M.C., 1997. Geology and Tectonic evolution of the Pontides: in A.G.Robinson, ed., Regional and petroleum geology of the Black Sea and surrounding region. AAPG Memoir 68, 183-226.

Yusoff, Z.M., Ngwenya, B.T., and Parsons, I. 2013. Mobility and fractionation of REEs during deep weathering of geochemically contrasting granites in a tropical setting, Malaysia. Chemical Geology, 349, 71–86.

Zhongxin, Y., Ge, B., Chenyu, W., Zhongqin, Z., Xianjiang, Y., 1992. Geological features and genesis of the Bayan Obo REE ore deposit, Inner Mongolia, China. Applied Geochemistry, 7, 429-442.

FIGURE CAPTIONS

Fig. 1: Main tectonic units of Turkey and the locations of the REE-bearing fluorite deposits.

Fig. 2: Schematic cross-sections of the REE-bearing fluorite deposits. **(a)** alkaline intrusive-hosted deposits (Bayındır, İsahocalı, Cangıllı, Akçakent and Divriği), **(b)** carbonate-hosted deposits (Keban, Akdağ, Pöhrenk,Tavşanlı, Akkaya and Yeşilyurt), **(c)** carbonatite-hosted deposits (Kızılcaören and Kuluncak). Bayındır, İsahocalı, Cangıllı and Akçakent deposits show similar host rock relationships and therefore are shown on a single section. (Bfro: Banded fluorite rich ore, Bmro : Banded manganese oxide rich ore, Bbro: Banded barite rich ore, Bs: Banded silica, Cs: Upper Cretaceous Serpentinite, Mp: Late Oligocene phonolite, Mam: Metasomatised alkaline magmatics, Pms: Paleozoic metasediments, UCl: Upper Cretaceous limestone, CPns: Upper Cretaceous- Lower Palaeocene nepheline syenite, Ts: Tertiary syenite, Tlp: Tertiary lamprophyre, c-q: Clay-quartz, Tag: Tertiary alkaline granite, aa: Argillic alteration, PTm: Permian-Triassic metamorphics, CPsp: Upper Cretaceous- Lower Palaeocene syenite porphyry, Pmr: Paleozoic marble, Pms: Paleozoic metasediments, Cgp: Upper Cretaceous granite porphyry, Mss: Miocene sandstone-shale, El: Eocene limestone, Csh: Upper Cretaceous shale, Cd: Upper Cretaceous diabase, Pl: Paleozoic limestone, F: Fluorite, Ba: Barite, Th: Thorium, REE: Rare Earth Element, Cu: Copper, Pb: Lead, Zn: Zinc).

Fig. 3: **(a)** Banded fluorite –rich ore with crosscutting vein indicates multiphase mineralization event, and **(b)** banded manganese oxide-rich ore with alkali silicate of the Kızılcaören REEs+Fluorite+Barite+Th deposit. (**c, d)** Kuluncak fluorite +REE deposit occurs as lenticular bodies with coarse crystallized and purple coloured fluorides.

Fig. 4: The fluorite ore veins associated with alkali intrusives: (**a, b)** Bayındır, **(c)** İsahocalı, **(d)** Cangıllı, (**e, f)** Akçakent, and **(g, h)** Divriği.

Fig. 5: Photos of carbonate-hosted fluorite ore bodies; **(a)** Keban, **(b)** Tad Deresi, **(c)** Akkaya, **(d)** Yeşilyurt, **(e)** Pöhrenk, and **(f)** Tavşanlı deposit. (slm: silisified limestone; Fl: fluorite; Ba: Barite).

Fig. 6: **(a)** Chondrite - normalised (Boynton, 1984) REE patterns for the mean values of the carbonatite-hosted Kızılcaören (KO) and Kuluncak (KUL) Fluorite+REEs deposits. **(b)** alkaline intrusive-hosted fluorite ores. **(c)** Chondrite-normalized (Boynton, 1984) REE patterns for mean values in carbonate-hosted fluorite ores.

Fig. 7: Photomicrograph of LV and LVS-type fluid inclusions of (a to c) intrusive-hosted, (d to g) carbonate-hosted and (h to j) carbonatite-hosted deposits. (a) LV and (b) LVS-type in Divriği; (c) LV-type in Akçakent ; (d) LV-type in Pöhrenk ; (e) LV-type and (f) LVS-type in Keban; (g) LV-type in Tavşanlı; (h and i) multisolid-bearing LVS-type in Kuluncak; and (j) multisolid-bearing LVS-type in Kızılcaören deposit. Scale bar is 20 µm for a, b, c; 10 µm for d, e, f, g, h, i and j.

Fig. 8: Distribution of Te (eutectic temp.), Tm-ice (last ice melting temp.), and Tm-clth (clathrate melting temp.) of LV and LVS-type inclusions in fluorite minerals of **(a)** carbonatite-hosted, **(b)** intrusive-hosted, and **(c)** carbonate-hosted deposits.

Fig. 9: Homogenization temperature histogram of **(a)** carbonatite-hosted deposits, **(b)** intrusive-hosted, **(c)** carbonate-hosted; and Th versus wt. % NaCl eq. diagram of **(d)** carbonatite-hosted, **(e)** intrusive-hosted, and (f) carbonate-hosted REE-bearing fluorite deposits of Turkey.

Fig. 10: Plots of fluorite-REE ore composition on Nb+Ta versus TREE diagram showing good differentiation as being high temperature deposits (carbonatite- hosted, alkali intrusive- hosted) and low temperature formed (carbonate- hosted) deposits.

Fig. 11: Tb/Ca vs. Tb/La diagram for carbonatite- hosted, alkali intrusive- hosted and carbonate-hosted REE-bearing fluorite deposits. Beyond the carbonatite-hosted Kızılcaören and Kuluncak deposit, the other REE-rich and high temperature formed deposits such as carbonate -hosted Keban and alkaline intrusive-hosted Divriği deposit also fall into the pegmatitic field. Scattering nature of the carbonate -hosted deposits from sedimentary to hydrothermal and pegmatite fields indicate their common source (Trends taken from O’Connor et al., 1993).

Fig. 12: Correlation coefficients between Eu and Rb, Ba, Ce, and Sr which were defined by correlation matrix for the REE-bearing fluorite deposits. A common negative r values

for Akkaya and positive r values for the Pöhrenk should be represent two end members, resembling the oxidizing and reducing formation condition, respectively. Variable negative and positive r values between Sr and Eu could be indicate Eu deposition from the fluids occurred both Eu^{+3} and Eu^{+2} form.

Fig. 13: Chondrite-normalized (Boynton, 1984) REE pattern (shadow area) of the studied REE-bearing fluorite formations of Turkey compared with other fluorite- REE deposits of the world. The Bayan Obo (China) REE data is taken from Xu et al., (2012) the South Platte (USA) fluorite deposit from Willams-Jones et al., (2000) and the La Encantada (Mexico) from Levresse et al., (2006).

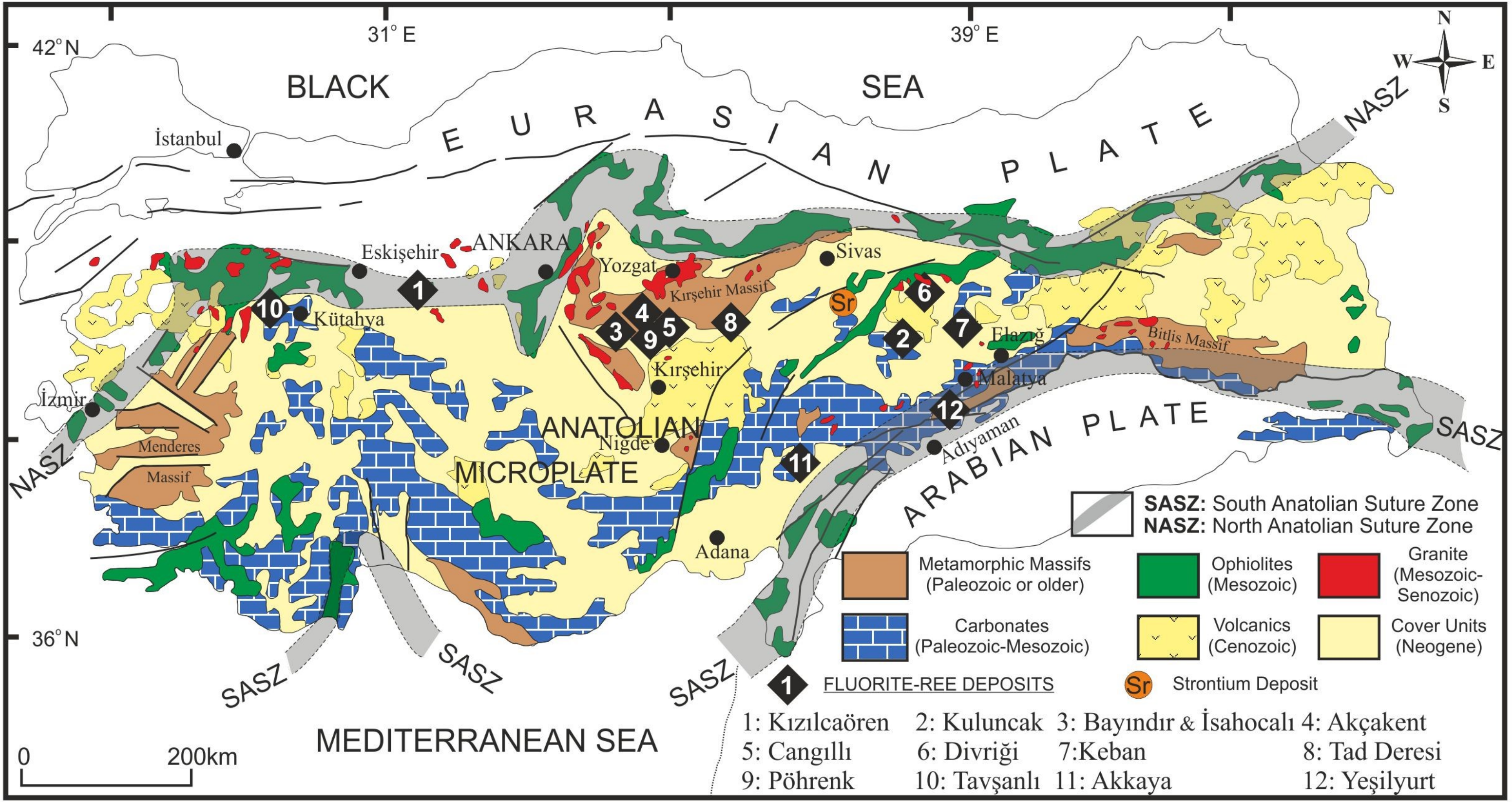

31° E
39° E
42° N
36° N
N
W
E
S
BLACK
SEA
EURASIAN PLATE
NASZ
İstanbul
Eskişehir
ANKARA
Yozgat
Sivas
Kırşehir Massif
Kütahya
Elazığ
Bitlis Massif
Kırşehir
Malatya
İzmir
Menderes
Massif
ANATOLIAN
MICROPLATE
Nigde
Adıyaman
ARABIAN PLATE
SASZ
Adana
Sr
1
2
3
4
5
6
7
8
9
10
11
12
SASZ: South Anatolian Suture Zone
NASZ: North Anatolian Suture Zone
Metamorphic Massifs (Paleozoic or older)
Ophiolites (Mesozoic)
Granite (Mesozoic-Senozoic)
Carbonates (Paleozoic-Mesozoic)
Volcanics (Cenozoic)
Cover Units (Neogene)
FLUORITE-REE DEPOSITS
Strontium Deposit
MEDITERRANEAN SEA
0
200km
1: Kızılcaören
2: Kuluncak
3: Bayındır & İsahocalı
4: Akçakent
5: Cangıllı
6: Divriği
7:Keban
8: Tad Deresi
9: Pöhrenk
10: Tavşanlı
11: Akkaya
12: Yeşilyurt

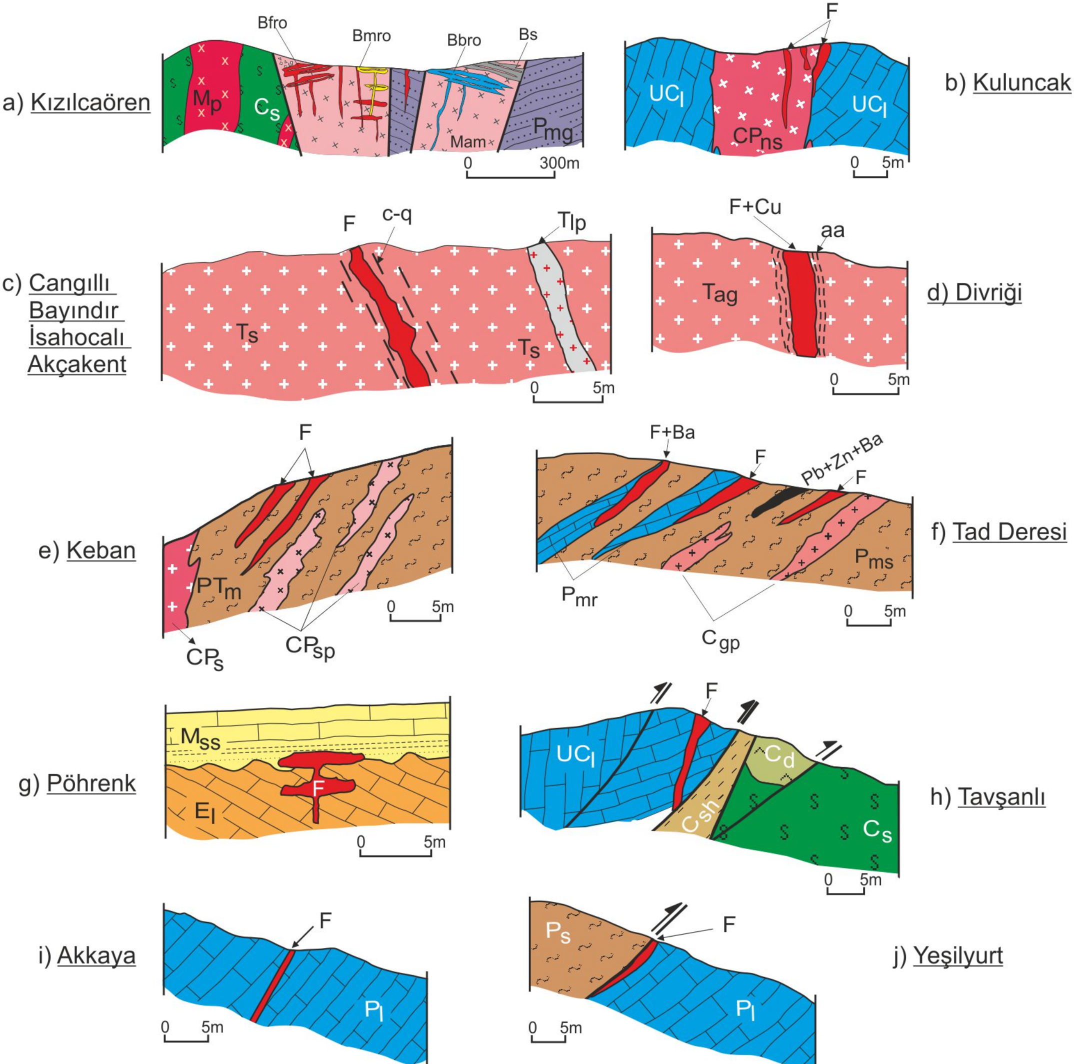

a) Kızılcaören
Bfro
Bmro
Bbro
Bs
Mp
Cs
Mam
Pmg
0 300m
b) Kuluncak
F
UCl
CPns
UCl
0 5m
c) Cangıllı
Bayındır
İsahocalı
Akçakent
F
c-q
Tlp
Ts
Ts
0 5m
d) Divriği
F+Cu
aa
Tag
0 5m
e) Keban
F
PTm
CPs
CPsp
0 5m
f) Tad Deresi
F+Ba
F
Pb+Zn+Ba
F
Pms
Pmr
Cgp
0 5m
g) Pöhrenk
Mss
F
El
0 5m
h) Tavşanlı
F
UCl
Cd
Csh
Cs
0 5m
i) Akkaya
F
Pl
0 5m
j) Yeşilyurt
Ps
F
Pl
0 5m

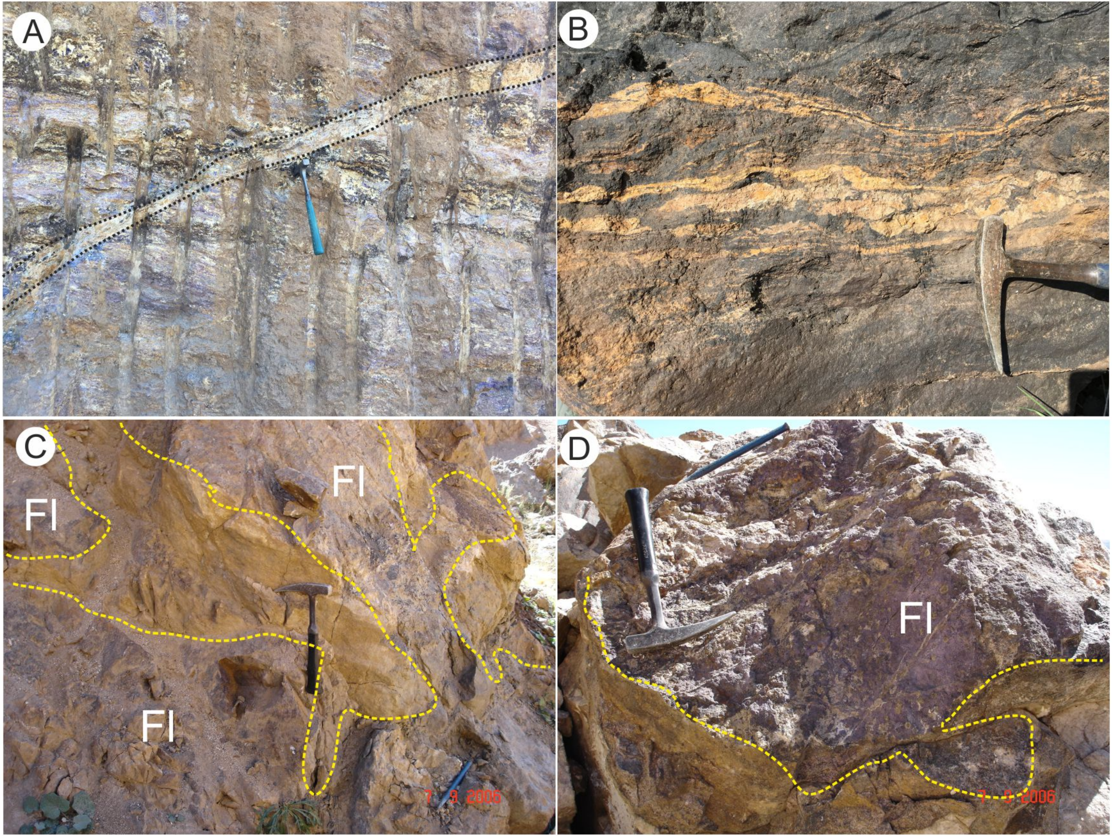
A
B
C
D
Fl
Fl
Fl
Fl
7 9 2006
7 9 2006

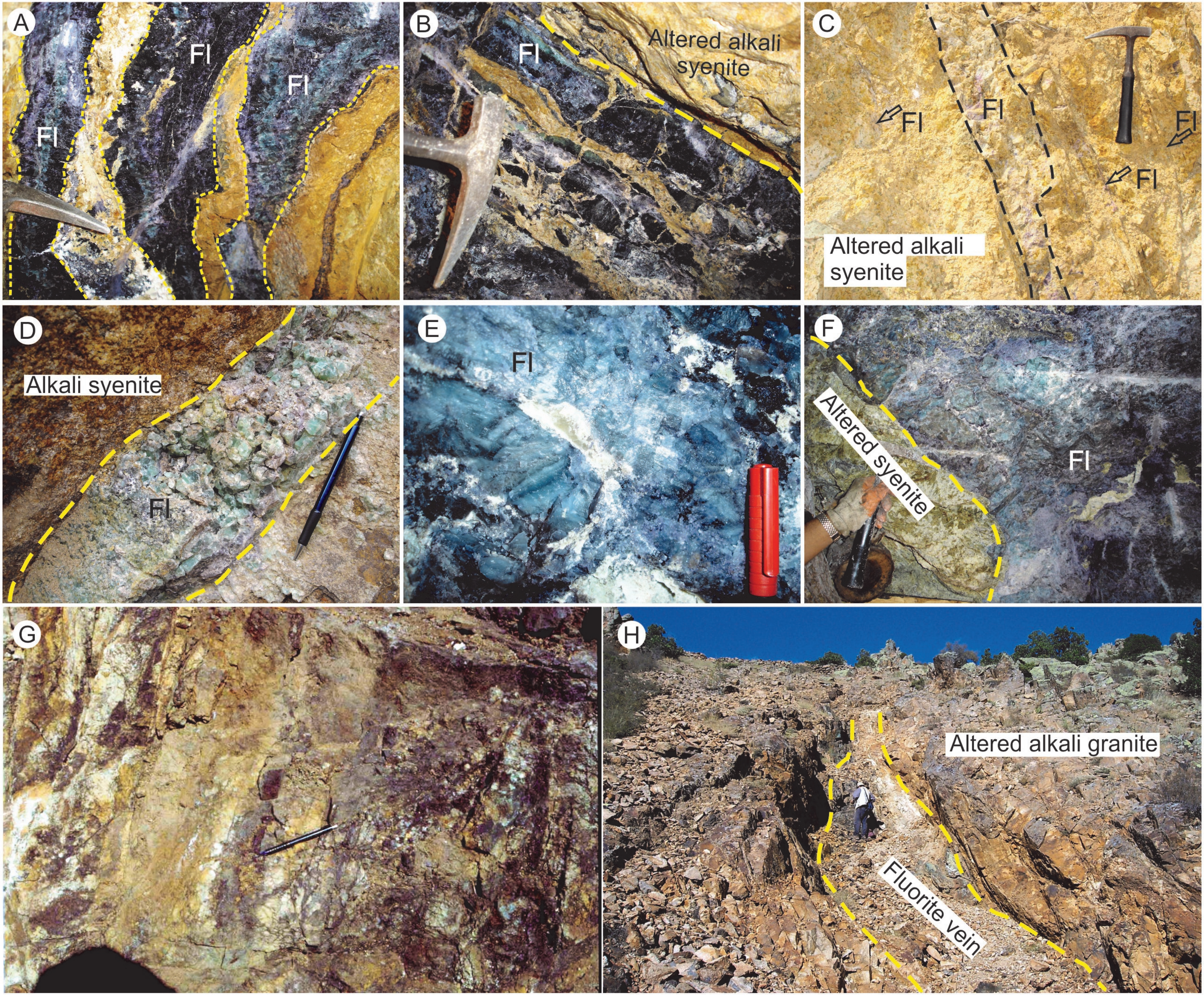
A
Fl
Fl
Fl
B
Fl
Altered alkali syenite
C
Fl
Fl
Fl
Fl
Altered alkali syenite
D
Alkali syenite
Fl
E
Fl
F
Altered syenite
Fl
G
H
Altered alkali granite
Fluorite vein

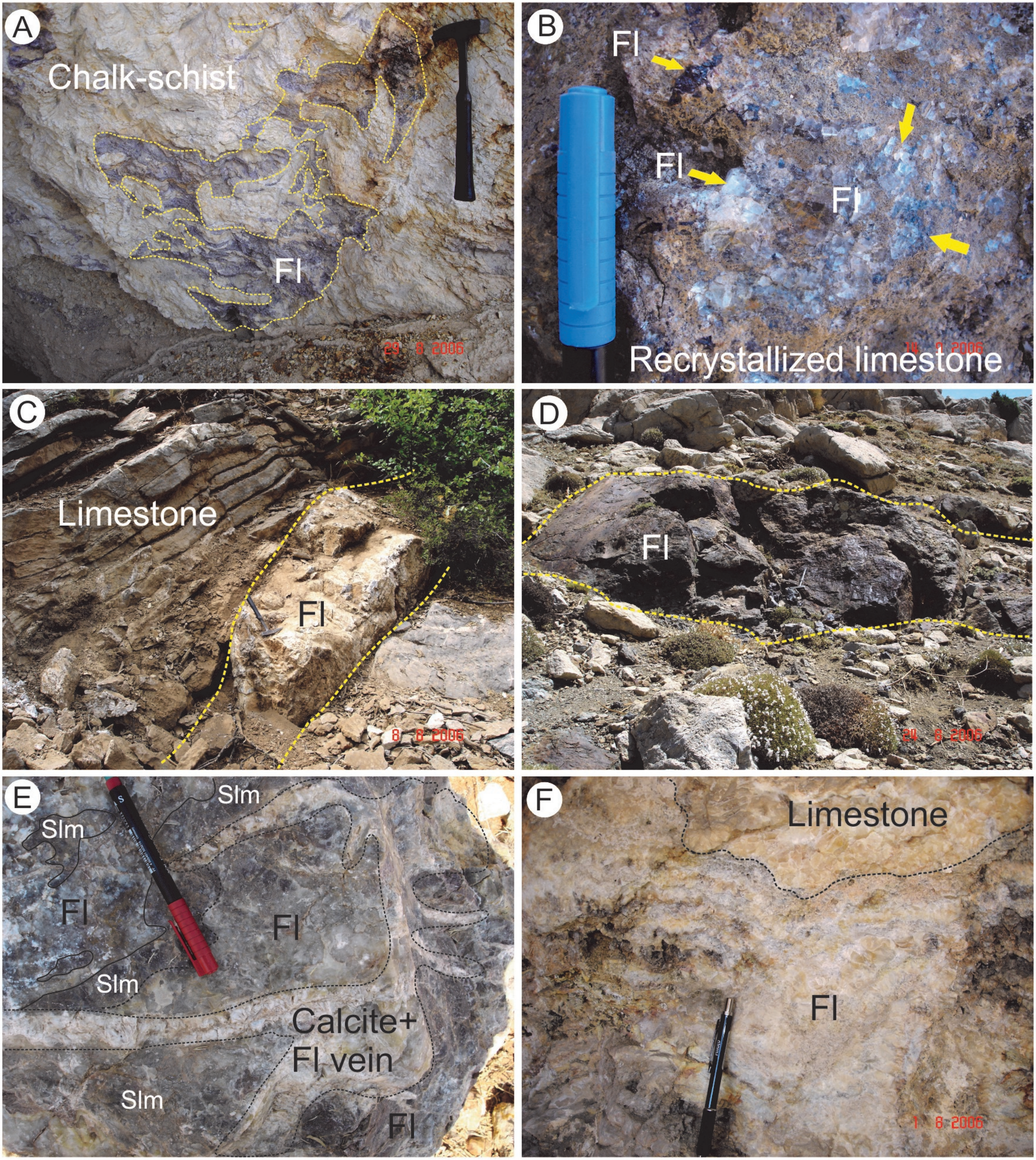
A
Chalk-schist
Fl
29 8 2006
B
Fl
Fl
Fl
Recrystallized limestone
C
Limestone
Fl
8 8 2006
D
Fl
24 8 2006
E
Slm
Slm
Fl
Fl
Slm
Calcite+
Fl vein
Slm
Fl
F
Limestone
Fl
1 8 2006

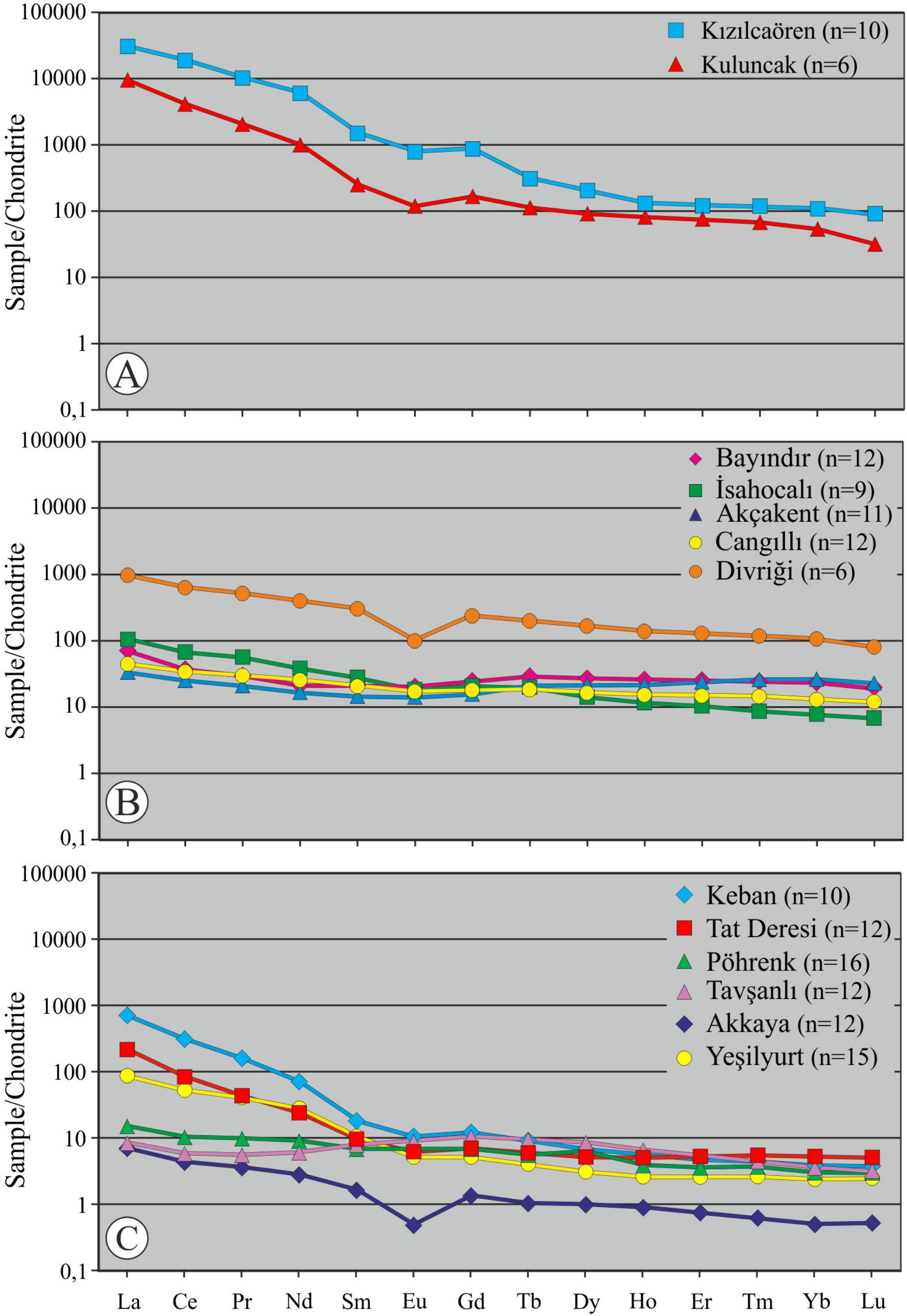

Kızılcaören (n=10)
Kuluncak (n=6)
Sample/Chondrite
100000
10000
1000
100
10
1
0,1
A
Bayındır (n=12)
İsahocalı (n=9)
Akçakent (n=11)
Cangıllı (n=12)
Divriği (n=6)
B
Keban (n=10)
Tat Deresi (n=12)
Pöhrenk (n=16)
Tavşanlı (n=12)
Akkaya (n=12)
Yeşilyurt (n=15)
C
La
Ce
Pr
Nd
Sm
Eu
Gd
Tb
Dy
Ho
Er
Tm
Yb
Lu

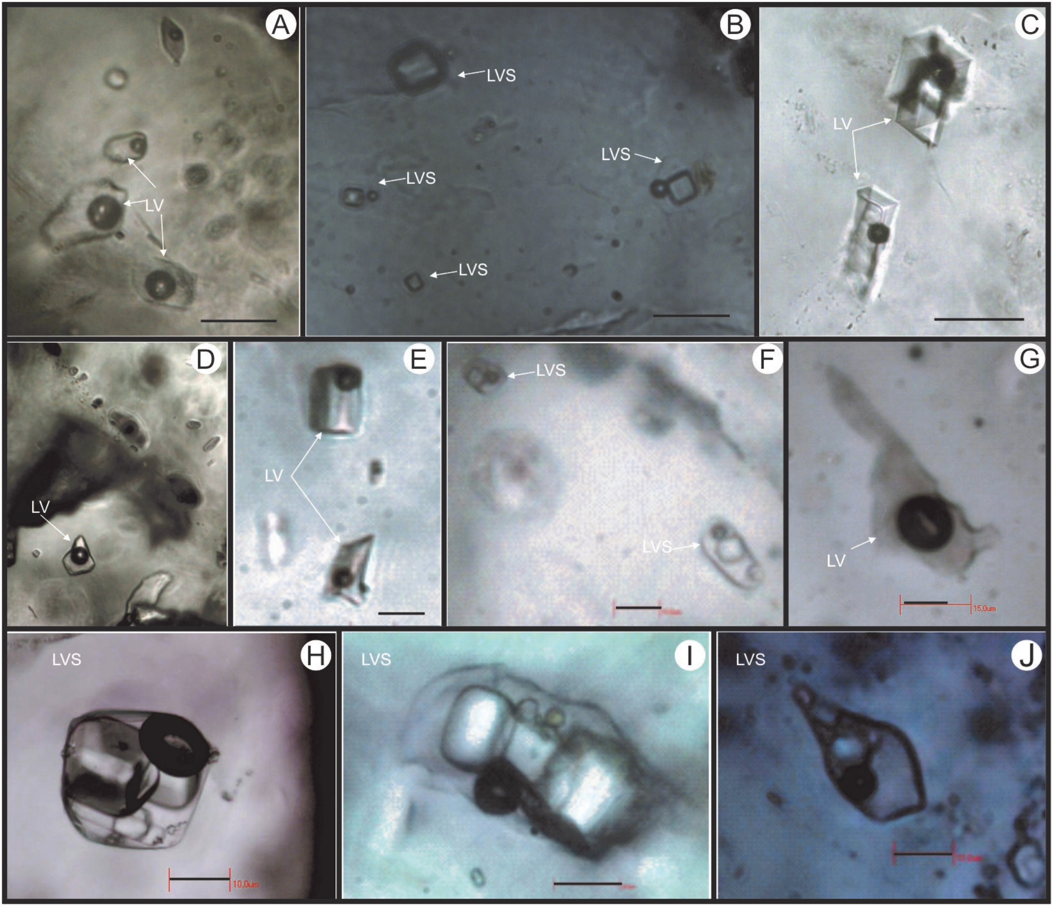
A
B
C
D
E
F
G
H
I
J
LV
LVS
15,0um
10,0um

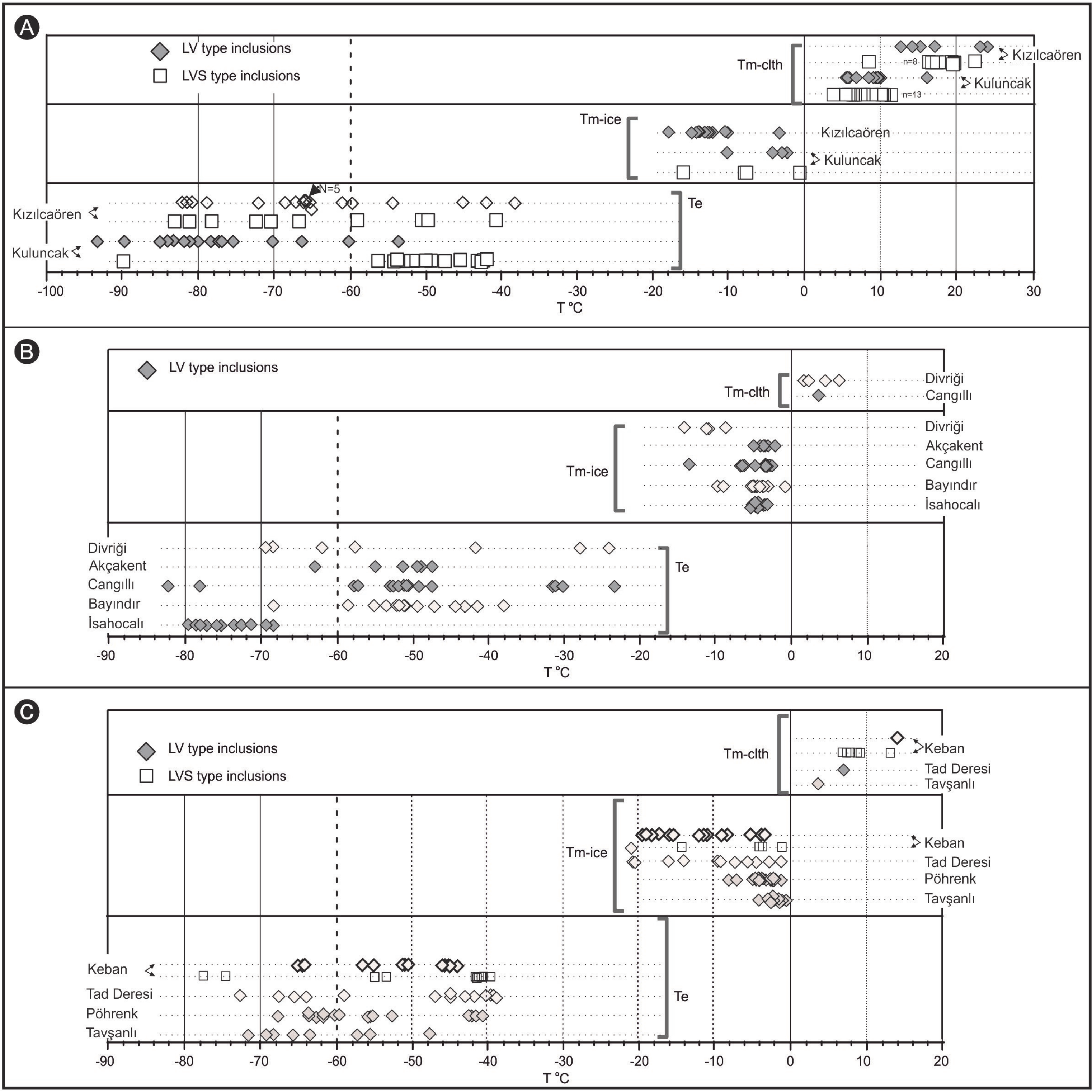
A
LV type inclusions
LVS type inclusions
Tm-clth
Kızılcaören
n=8
Kuluncak
n=13
Tm-ice
Kızılcaören
Kuluncak
N=5
Te
Kızılcaören
Kuluncak
-100 -90 -80 -70 -60 -50 -40 -30 -20 -10 0 10 20 30
T °C
B
LV type inclusions
Tm-clth
Divriği
Cangıllı
Tm-ice
Divriği
Akçakent
Cangıllı
Bayındır
İsahocalı
Te
Divriği
Akçakent
Cangıllı
Bayındır
İsahocalı
-90 -80 -70 -60 -50 -40 -30 -20 -10 0 10 20
T °C
C
LV type inclusions
LVS type inclusions
Tm-clth
Keban
Tad Deresi
Tavşanlı
Tm-ice
Keban
Tad Deresi
Pöhrenk
Tavşanlı
Te
Keban
Tad Deresi
Pöhrenk
Tavşanlı
-90 -80 -70 -60 -50 -40 -30 -20 -10 0 10 20
T °C

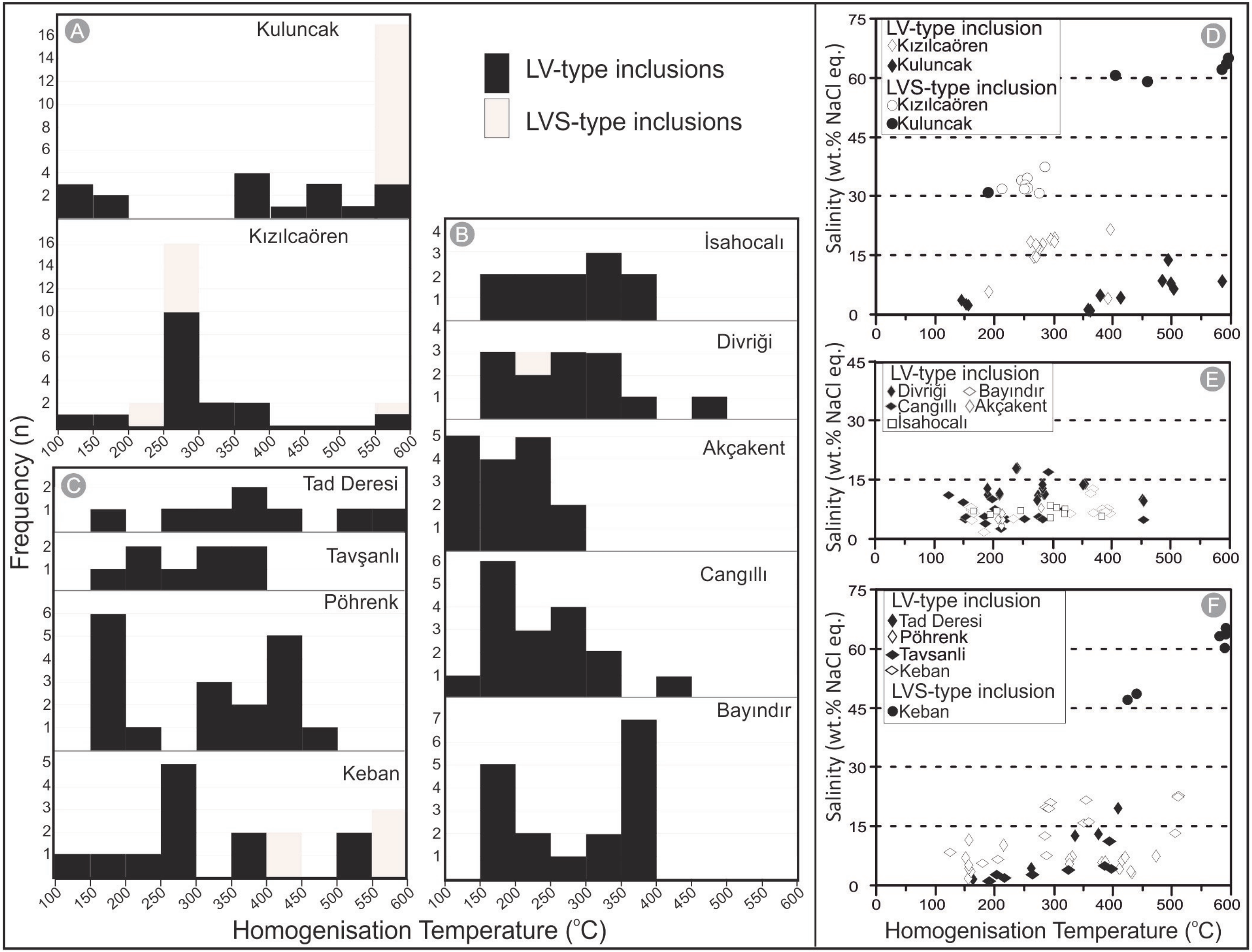
A
Kuluncak
Kızılcaören
LV-type inclusions
LVS-type inclusions
B
İsahocalı
Divriği
Akçakent
Cangıllı
Bayındır
C
Tad Deresi
Tavşanlı
Pöhrenk
Keban
Frequency (n)
Homogenisation Temperature (°C)
D
LV-type inclusion
Kızılcaören
Kuluncak
LVS-type inclusion
Kızılcaören
Kuluncak
Salinity (wt.% NaCl eq.)
E
LV-type inclusion
Divriği
Bayındır
Cangıllı
Akçakent
İsahocalı
F
LV-type inclusion
Tad Deresi
Pöhrenk
Tavsanli
Keban
LVS-type inclusion
Keban
Homogenisation Temperature (°C)

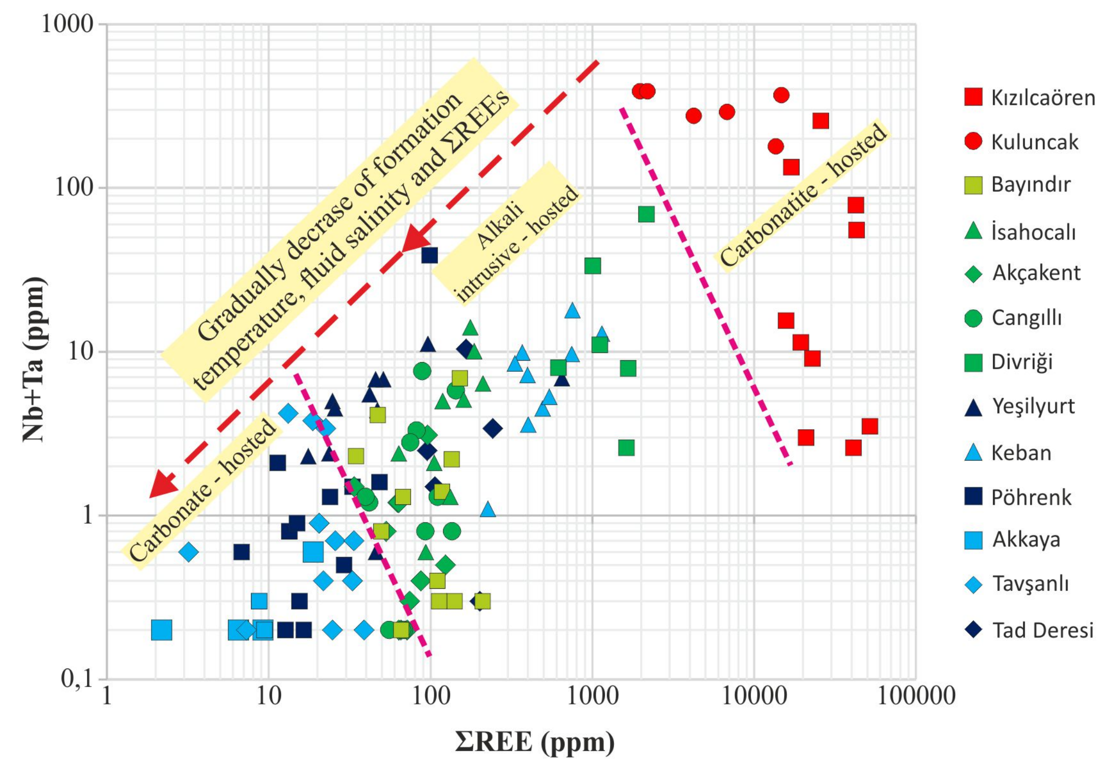
Gradually decrase of formation temperature, fluid salinity and ΣREEs
Alkali intrusive - hosted
Carbonatite - hosted
Carbonate - hosted
Nb+Ta (ppm)
ΣREE (ppm)
1000
100
10
1
0,1
1
10
100
1000
10000
100000
Kızılcaören
Kuluncak
Bayındır
İsahocalı
Akçakent
Cangıllı
Divriği
Yeşilyurt
Keban
Pöhrenk
Akkaya
Tavşanlı
Tad Deresi

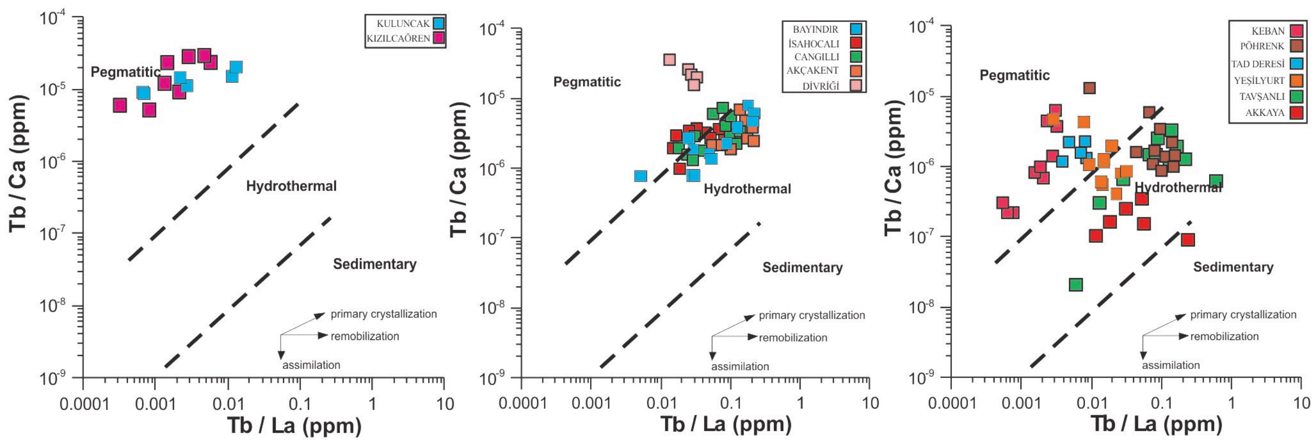

KULUNCAK
KIZILCAÖREN
Pegmatitic
Hydrothermal
Sedimentary
primary crystallization
remobilization
assimilation
Tb / Ca (ppm)
Tb / La (ppm)
BAYINDIR
İSAHOCALI
CANGILLI
AKÇAKENT
DİVRİĞİ
Pegmatitic
Hydrothermal
Sedimentary
primary crystallization
remobilization
assimilation
Tb / Ca (ppm)
Tb / La (ppm)
KEBAN
PÖHRENK
TAD DERESİ
YEŞİLYURT
TAVŞANLI
AKKAYA
Pegmatitic
Hydrothermal
Sedimentary
primary crystallization
remobilization
assimilation
Tb / Ca (ppm)
Tb / La (ppm)

Deposits	Rb	Ba	Ce	Sr
Kızılcaören	-0.58	0.66	-0.24	-0.10
Kuluncak	0.14	-0.64	0.28	0.38
Bayındır	-0.31	-0.07	0.29	0.79
İsahocalı	**-0.08**	**-0.16**	**0.39**	**-0.84**
Cangıllı	0.26	0.31	0.42	-0.18
Akçakent	-0.57	0.23	0.49	0.74
Divriği	0.34	0.06	0.94	-0.51
Keban	0.72	0.52	0.88	-0.71
Tad Deresi	-0.82	-0.70	0.97	0.08
Pöhrenk	**0.71**	**0.89**	**0.39**	**0.89**
Tavşanlı	-0.18	0.40	0.03	0.21
Akkaya	**-0.50**	**-0.64**	**-0.22**	**-0.59**
Yeşilyurt	0.16	-0.06	1.00	-0.16

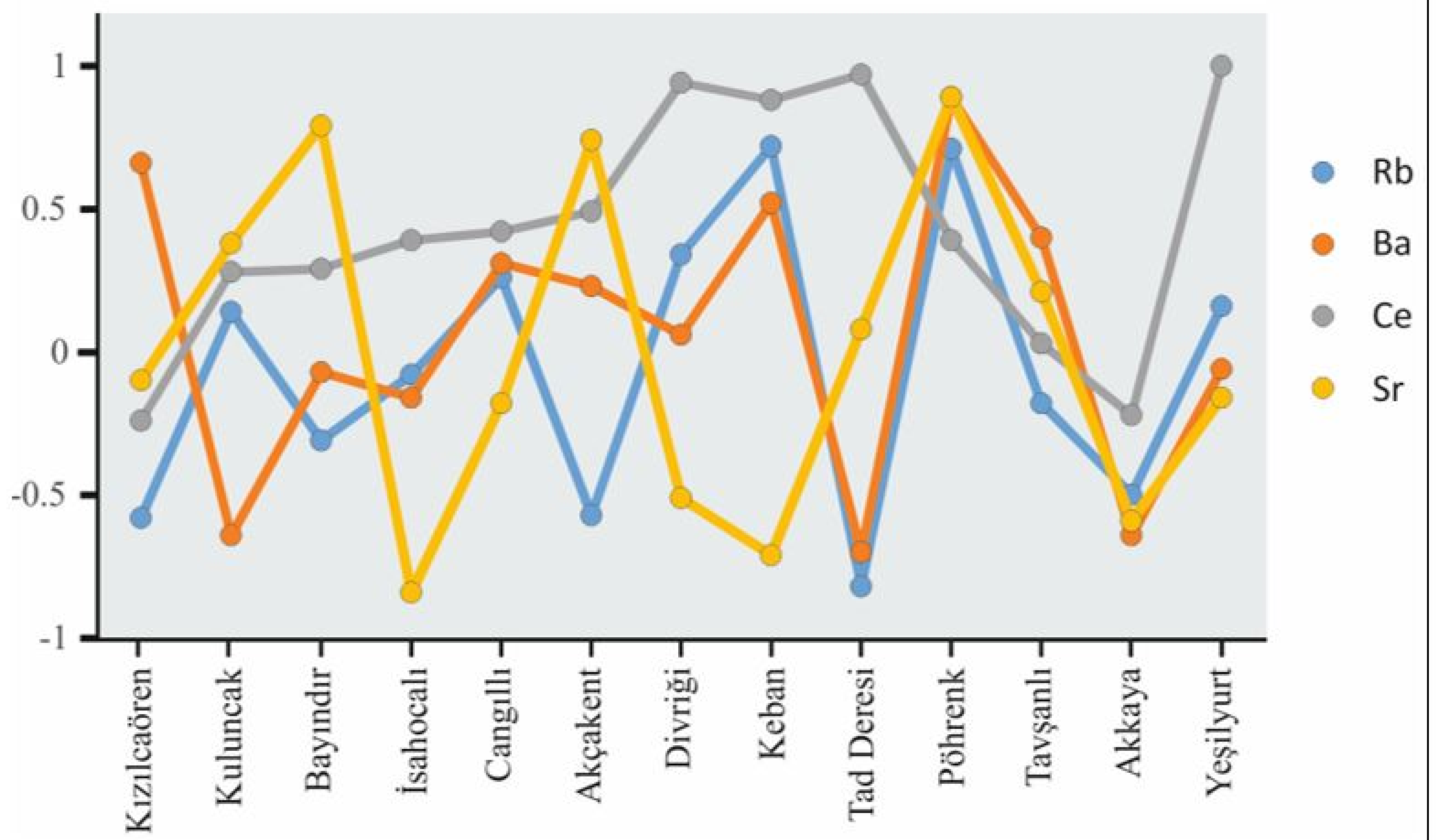

Figure 13

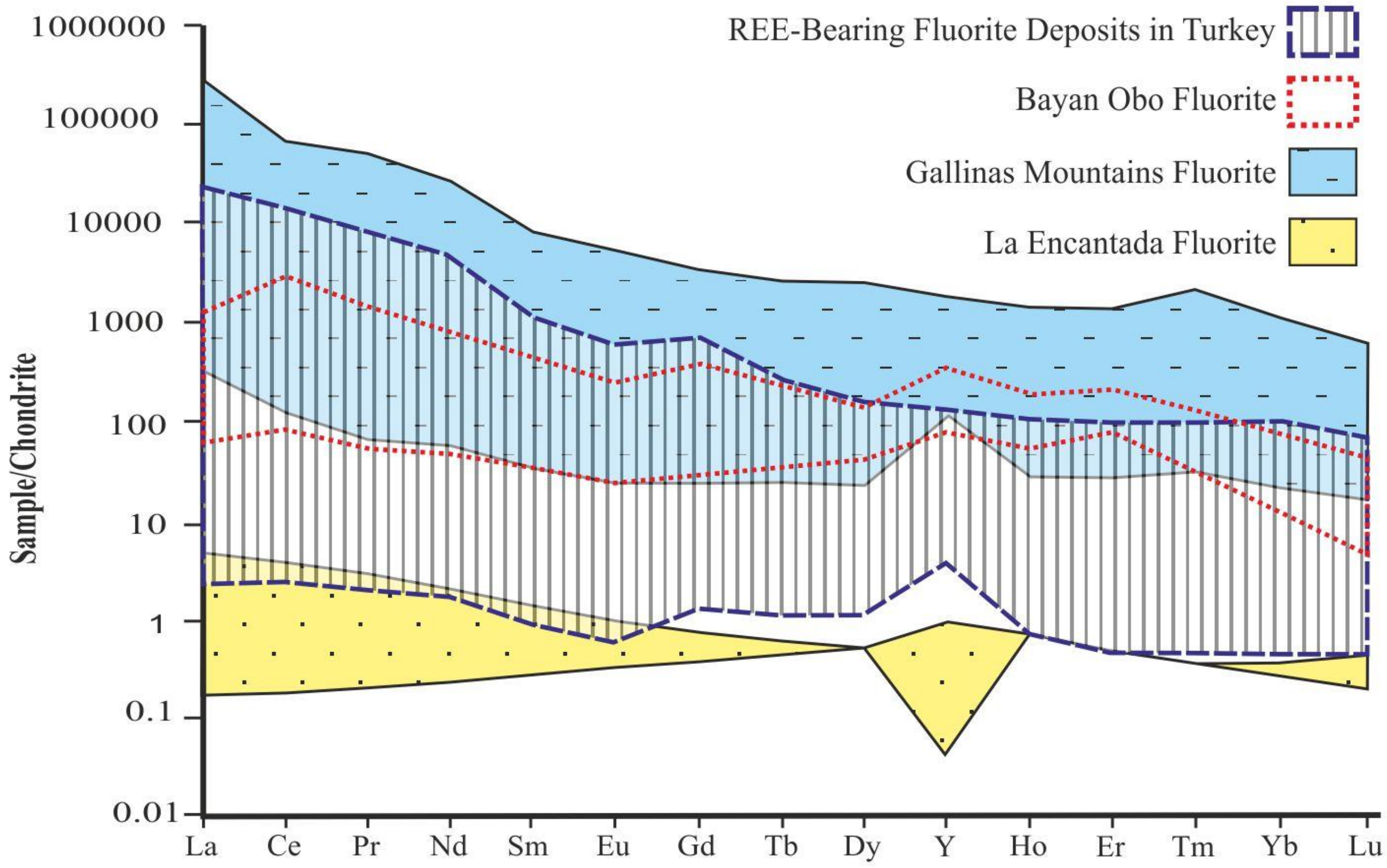
REE-Bearing Fluorite Deposits in Turkey
Bayan Obo Fluorite
Gallinas Mountains Fluorite
La Encantada Fluorite
Sample/Chondrite
1000000
100000
10000
1000
100
10
1
0.1
0.01
La
Ce
Pr
Nd
Sm
Eu
Gd
Tb
Dy
Y
Ho
Er
Tm
Yb
Lu